

國立臺灣大學電機資訊學院資訊網路與多媒體研究所



博士論文

Graduate Institute of Networking and Multimedia
College of Electrical Engineering and Computer Science
National Taiwan University
Doctoral Dissertation

睡眠事件之偵測與瀏覽

On Detection and Browsing of Sleep Events

陳昭伶

Chao-Ling Chen

指導教授：洪一平 博士

Advisor: Yi-Ping Hung, Ph.D.

中華民國 105 年 6 月

June, 2016



國立臺灣大學博士學位論文
口試委員會審定書

睡眠事件之偵測與瀏覽

On Detection and Browsing of Sleep Events

本論文係陳昭伶君（學號 D96944006）在國立臺灣大學資訊網路與多媒體研究所完成之博士學位論文，於民國一百零五年六月六日承下列考試委員審查通過及口試及格，特此證明

口試委員：

洪平

（簽名）

（指導教授）

賴希安

陳永昇

廖云輝

陳冠文

逄愛君

所長：



致謝

感謝指導教授洪一平老師及冠文學長，在研究過程的指導與幫助。感謝口試委員賴飛熊老師、陳永昇老師、唐玄輝老師及陳冠文老師，所提供的寶貴建議。感謝延瑜、家翰、力韋、建男、偉齊、婷婷、瑋倫、亮均、威翰、千嘉、喬偉、經堯、志聰、鴻勳、文慶、兆哲、永祥、士堯、志瑋、禾淋和欣倩，度過充滿樂趣的求學生涯。感謝家人的支持與鼓勵。感謝在這段期間，成就此論文的一切因緣。



摘要

本研究的目的，在提供睡眠自我檢測的客觀量測工具，並提出應用於蓋被情境的睡姿辨識方法。醫學上的睡眠多項生理檢查，需要使用接觸式的設備，取得生理訊號資訊；然而接觸式的設備可能影響睡眠，且檢查的費用昂貴。本研究設計非接觸式的睡眠瀏覽系統，採用普及的深度攝影機設備，方便於居家使用。目前採用影像處理的睡姿辨識方法，在未蓋被情況下進行睡姿分類，無法應用於真實睡眠情境。使用深度影像的三維訊息，本研究實現在蓋被情況下進行睡姿辨識的方法。

本研究提出時間區間的方法用於偵測睡眠事件，基於深度資訊的睡姿辨識方法用於分類睡姿。睡眠瀏覽系統採用具有多重感測器的裝置，偵測床上的使用者及周遭環境中發生的睡眠事件。裝置包含紅外線深度感測器、彩色攝影機及麥克風陣列，分別偵測三種睡眠事件：動作事件、光照事件及聲音事件。由輸入的深度訊號流及彩色影像流，系統建立背景模型，偵測動作變化及光照變化，並同步量化三種訊號。當訊號分數超過各別的實驗門檻值，即觸發時間區間的方法，紀錄各別的睡眠事件，紀錄的內容包含深度影像、彩色影像及聲音檔案。系統提供睡眠歷程的瀏覽介面，呈現睡眠事件的分數曲線及整合後的影音檔案。睡姿偵測的方法分類四種睡姿類別：左側睡、右側睡、平躺及趴睡；其中左側睡及右側睡包含胎兒型、思念型及木頭型睡姿，平躺包含軍人型及海星型睡姿，趴睡包含木頭型和自由落體型睡姿。在實驗前測階段，為了計算床平面，將記錄空床的深度影像轉換為世界座標系。將每張記錄使用者的深度影像轉換為世界座標系，計算每個深度點至床平面的距離。將每張深度影像的距離陣列做為輸入，採用支持向量機的機器學習方法，實現睡姿分類。實驗模擬真實睡眠情

境，在三種條件下進行，沒蓋被狀態、蓋薄被狀態及蓋厚被狀態。

本研究結果顯示：（1）睡眠瀏覽系統具有效率及可靠性，使用者透過本系統快速瀏覽睡眠事件紀錄，並經由觀看影片檢視睡眠事件的內容。（2）睡姿辨識方法在厚被的條件下，比未蓋被和薄毯的條件下有更好的辨識結果，因為厚被的厚度增強睡姿動作的特徵。本研究的發現可作為未來在居家情境中，進行睡眠事件偵測及睡姿辨識研究的指南。

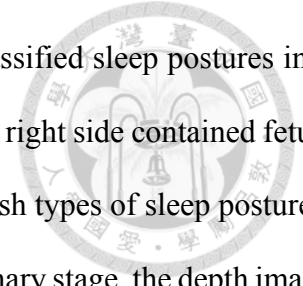
關鍵詞：深度影像、影像序列分析、睡眠瀏覽、非接觸式睡眠事件偵測、睡姿辨識。



ABSTRACT

The purpose of the study was to provide an objective measurement tool for sleep self-examination, and to propose a method for sleep posture recognition of a subject under covering. Polysomnography (PSG) in clinical therapy requires attached devices to obtain bioinformation; however, the attached devices may result in uncomfortable sleeping, and the cost of the examination is expensive. In the study, using a common depth camera device, an unconstrained sleep browsing system has been developed for applying to home scenario. Current methods based on image processing technique in sleep posture recognition, classified sleep postures in the condition of a subject without covering, and were unable to apply to real sleep scenario. Using three-dimensional information of depth image, a method of sleep posture recognition was realized in the condition of a subject under covering.

In the study, epoch method was proposed for recording sleep events, and a method of sleep posture recognition based on depth image was proposed for classifying sleep postures. Using a device with multiple sensors, the sleep browsing system detected sleep events from a subject in bed and the surrounding environment. Based on the multiple sensors of the device, including an infrared depth camera, a color camera, and a four-microphone array, three types of sleep events were detected: motion event, lighting event and sound event. From the input of depth image stream and the input of color image stream, background modeling in the system was used to measure body movements and lighting changes, and the three types of signals were quantified simultaneously. When type of signal score was greater than each empirical threshold, the epoch method was triggered for recording independent sleep events, and the recording contained depth images, color images and audio files. The system provided a browsing interface with sleep diagram, presenting the score curves of sleep



events and integrated videos. The method of sleep posture recognition classified sleep postures into four classes: left side, right side, supine and stomach, in which left side and right side contained fetus, yearner and log types of sleep postures, supine contained soldier and starfish types of sleep postures, and stomach contained log and freefaller types of sleep postures. In preliminary stage, the depth image capturing an empty bed was transformed into world coordinate for calculating the bed plane. Each depth image capturing a subject was transformed into world coordinate, and the vertical distance of each depth pixel to the bed plane was calculated. From the input distance array of each depth image, the Support Vector Machine (SVM) method was adopted for classifying sleep postures. Experiments for simulating real sleep scenario with three conditions were carried out: without covering condition, blanket covering condition and quilt covering condition.

The survey concluded: (1) The sleep browsing system had efficiency and reliability that users browsed the recording of sleep events efficiently, and examined the content of sleep events by watching the videos. (2) The method of sleep posture recognition had a better performance in quilt covering condition than without covering condition and blanket covering condition, because the layer of quilt enhances the features of sleep postures. The study findings may serve as a guide for future research on sleep event detection and sleep posture recognition in home scenario.

Keywords: Depth image, image sequence analysis, sleep browsing, unconstrained sleep event detection, sleep posture recognition.



TABLE OF CONTENTS

口試委員審定書.....	i
致謝	ii
摘要	iii
ABSTRACT	v
TABLE OF CONTENTS.....	vii
TABLE OF FIGURES	x
TABLE OF TABLES	xii
CHAPTER 1 INTRODUCTION	1
1.1 Background and Motivation.....	1
1.2 Outline of this Research	3
1.2.1 Sleep Browsing System for Sleep Event Detection and Browsing	3
1.2.2 Sleep Posture Recognition Based on Depth Image.....	3
1.3 Organization of the Dissertation	4
CHAPTER 2 RELATED WORK.....	5
2.1 Constrained versus Unconstrained Sleep Detection	5
2.2 Constrained versus Unconstrained Sleep Posture Recognition	6
2.3 Summary	8



CHAPTER 3 SLEEP BROWSING SYSTEM FOR SLEEP EVENT

DETECTION AND BROWSING.....	9
3.1 Sleep Event Type	9
3.2 System Overview	10
3.2.1 System Setup	10
3.2.2 System Flow	11
3.3 Sleep Event Detection and Recording.....	11
3.3.1 Background Modeling.....	12
3.3.2 Empirical Threshold of Sleep Event	13
3.3.3 Motion Threshold Adjustment	14
3.3.4 Epoch Method	15
3.3.5 Sleep Diagram for Browsing Sleep Events.....	17
3.4 Experiments on Overnight Sleep	19
3.4.1 Sleep/Wake Identification.....	20
3.4.2 Experiments on Discovering Sleep Events	21
3.4.3 Experiments on Sleep Quality Evaluation	23
3.5 Summary	28

CHAPTER 4 SLEEP POSTURE RECOGNITION BASED ON DEPTH IMAGE

.....	29
4.1 Sleep Posture Type.....	29
4.2 Sleep Posture Recognition	29



4.3 Experiments on Sleep Posture Recognition	30
4.3.1 Experimental Setup	31
4.3.2 Sleep Posture Feature	31
4.3.3 36-fold Cross Validation	37
4.4 Summary	50
CHAPTER 5 CONCLUSION AND FUTURE WORK.....	52
5.1 Summary of the Dissertation.....	52
5.2 Future Directions.....	53
LIST OF REFERENCES	54



TABLE OF FIGURES

Figure 3.1: Relationship between sensor and sleep event.....	10
Figure 3.2: An illustration of device setting.....	10
Figure 3.3: Flow chart of sleep browsing system.	11
Figure 3.4: Background modeling for measuring body movements and lighting changes.	12
Figure 3.5: Rescoring rule for correcting lighting score (Blue: motion event, green: lighting event and red: sound event).	14
Figure 3.6: Detection interface of sleep browsing system.	15
Figure 3.7: Epoch method.	17
Figure 3.8: Browsing interface of sleep browsing system: (a) Default threshold of each sleep event representing in black horizontal line, (b) and (c) Checkbox on the top for browsing and adjusting threshold of each sleep event independently, (d) Threshold of each sleep event representing in color horizontal line (Blue: motion event, green: lighting event and red: sound event).	19
Figure 3.9: Samples of sleep diagrams: (a) Participant A, (b) Participant B, (c) Participant C, (d) Participant D and (e) Participant E (Blue: motion event, green: lighting event and red: sound event).	23
Figure 3.10: Distribution of motion event (Blue: motion event, green: lighting event and red: sound event).	26
Figure 3.11: Samples of sleep diagrams: (a) Participant L, (b) Participant Q and (c) Participant R (Blue: motion event, green: lighting event and red: sound event).	27
Figure 4.1: Sleep posture type.....	29

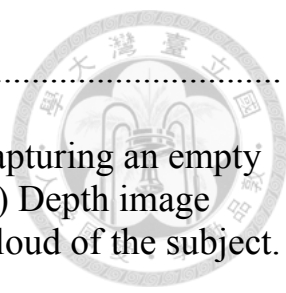


Figure 4.2: Steps of sleep posture recognition..... 30

Figure 4.3: World coordinate transformation: (a) Depth image capturing an empty bed, (b) ROI region of the bed, (c) 3D point cloud of the bed; (d) Depth image capturing a subject, (e) ROI region of the subject, (f) 3D point cloud of the subject. 30

Figure 4.4: Sleep posture experiments in three conditions: (a) Without covering condition, (b) Blanket covering condition and (c) Quilt covering condition..... 31

Figure 4.5: Features of left fetus class: (a) User 1 in without covering condition, (b) User 4 in blanket covering condition, and (c) User 11 in quilt covering condition.... 32

Figure 4.6: Features of right fetus class: (a) User 3 in without covering condition, (b) User 9 in blanket covering condition, and (c) User 10 in quilt covering condition.... 33

Figure 4.7: Features of left yearner class: (a) User 5 in without covering condition, (b) User 11 in blanket covering condition and (c) User 1 in quilt covering condition. 33

Figure 4.8: Features of right yearner class: (a) User 2 in without covering condition, (b) User 4 in blanket covering condition, and (c) User 10 in quilt covering condition. 34

Figure 4.9: Features of left log class: (a) User 2 in without covering condition, (b) User 18 in blanket covering condition and (c) User 4 in quilt covering condition..... 34

Figure 4.10: Features of right log class: (a) User 3 in without covering condition, (b) User 18 in blanket covering condition and (c) User 9 in quilt covering condition..... 35

Figure 4.11: Features of soldier class: (a) User 3 in without covering condition, (b) User 2 in blanket covering condition and (c) User 1 in quilt covering condition..... 35

Figure 4.12: Features of stomach log class: (a) User 5 in without covering condition, (b) User 11 in blanket covering condition and (c) User 1 in quilt covering condition. 36

Figure 4.13: Features of starfish class (a) User 2 in without covering condition, (b) User 3 in blanket covering condition and (c) User 1 in quilt covering condition..... 36

Figure 4.14: Features of freefaller class (a) User 2 in without covering condition, (b) User 3 in blanket covering condition and (c) User 3 in quilt covering condition..... 37



TABLE OF TABLES

Table 3.1: Comparison of sleep/wake identification algorithms.....	20
Table 3.2: Sleep parameters of overnight sleep experiments.....	21
Table 3.3: Sleep parameters of overnight sleep experiments.....	25
Table 4.1: 36-fold cross validation in three conditions.....	37
Table 4.2: 36-fold cross validation in without covering condition.	38
Table 4.3: Left side class and right side class with low accuracy in without covering condition.....	40
Table 4.4: Supine class and stomach class with low accuracy in without covering condition.....	41
Table 4.5: 36-fold cross validation in blanket covering condition.....	42
Table 4.6: Left side class and right side class with low accuracy in blanket covering condition.....	45
Table 4.7: Supine class and stomach class with low accuracy in blanket covering condition.....	45
Table 4.8: 36-fold cross validation in quilt covering condition.	46
Table 4.9: Left side class and right side class with low accuracy in quilt covering condition.....	49
Table 4.10: Supine class and stomach class with low accuracy in quilt covering condition.....	49



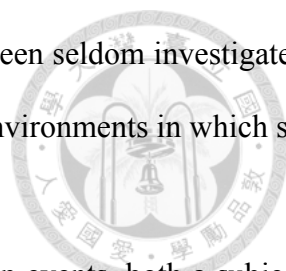
CHAPTER 1

INTRODUCTION

1.1 Background and Motivation

Since the World Association of Sleep Medicine (WASM) announced the World Sleep Day on March 14 to arise the attention from public to sleep issues in 2008, and how to improve better sleep experience has become a critical research topic in both academia and clinical fields. Traditionally, Polysomnography (PSG) has been used as the gold standard in clinical therapy measuring brain waves, muscle tone, eye movements, breathing patterns and blood oxygen levels with many electrodes, pressure transducers, a pulse oximeter and a sound probe. However, the attached devices may result in uncomfortable sleeping. For reducing the requirement of devices in sleep examination, many sleep detection methods had been proposed, including constrained and unconstrained methods. Constrained method in sleep detection used a ring with an accelerometer, some combining with lighting sensor or temperature sensor, and unconstrained method aimed to remove any contact on a subject using a pressure mattress or image processing technique. The purpose of these detection methods was to acquire sleep information of a subject in bed, such as frequency of turning behavior and respiratory cycle.

People are unaware of what exactly happened in the sleep environment during sleeping, and they feel the need to be assured their sleep in good sleep condition. For instance, when noises from outside traffic occur, the sound of the sleep event must be observed, and the afterward information like the reaction of the subject in bed must be captured. However, people are unable to get the information from

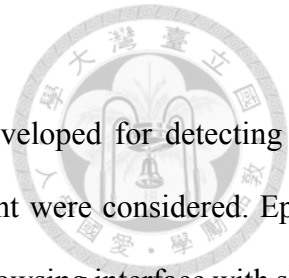


current sleep detection methods. To our best knowledge, this problem has been seldom investigated in the literature. Hence, a sleep browsing system is required in diverse sleep environments in which sleep events must be detected and concurrently captured.

To construct a sleep browsing system for detecting and recording sleep events, both a subject in bed and the sleep environment are considered, and the sensors of a depth camera, a color camera and a microphone are required. Recently, the commercial products embedded with a depth camera have become popular, and the price have decreased. In the study, Kinect for Windows combining with multiple sensors was used to detect sleep events, and a browsing interface with sleep diagram was provided for examining sleep.

Sleep posture is related to sleep quality and health. Some researches in clinical field had declared that a lateral posture is better than a supine posture to patients with sleep apnea [1] [2]. The evidence had shown that twice as high apnea index occurs when people sleep on their backs than side posture [3]. In addition, a supine posture may result in cessation of breathing when people are snoring, and a lateral posture is also helpful for preventing snoring [4]. A right side posture is good for health than the left lateral posture with less pressure on heart, especially for patients with heart disease [5]. For recognizing sleep postures, many researches with constrained and unconstrained methods had been proposed. Constrained method used a heart pressure sensor or a ring with an accelerometer, and unconstrained method chose a pressure mattress or image processing technique for classifying sleep postures. The challenge of the method based on image processing technique had difficulty to classify sleep postures with a subject under covering, and that was unable to practice in real sleep scenario. Besides, the pressure mattress is still not popular for the cost is expensive. In the study, an unconstrained method was proposed in sleep posture recognition considering the condition of a subject under covering.

1.2 Outline of this Research



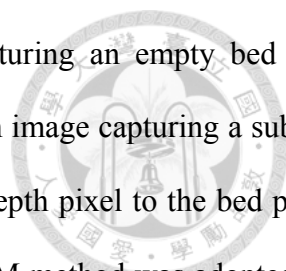
In this dissertation, an unconstrained sleep browsing system has been developed for detecting and browsing sleep events, and both a subject in bed and the sleep environment were considered. Epoch method was proposed for recording sleep events continuously, and a sleep browsing interface with sleep diagram was provided for browsing sleep. A method of sleep posture recognition based on depth image was proposed for applying to a subject under covering, and the Support Vector Machine (SVM) method was adopted to classify sleep postures into four classes.

1.2.1 Sleep Browsing System for Sleep Event Detection and Browsing

A sleep browsing system has been developed for detecting and browsing motion event, lighting event and sound event. To our best knowledge, the system is the first sleep browsing system for detecting sleep events considering environmental effects [8]. From the input of depth image stream and the input of color image stream, background modeling was used to quantify body movements and lighting changes. To better understanding the motion behaviors of sleep, the entire body region was considered. The body movements, lighting changes, and sounds were scored simultaneously. Epoch method was proposed for recording sleep events, containing depth images, color images and audio files. Finally, a browsing interface with sleep diagram was provided for browsing sleep events. Overnight sleep experiments for two weeks were carried out, and experimental results showed the efficiency and reliability of the sleep browsing system.

1.2.2 Sleep Posture Recognition Based on Depth Image

An unconstrained method based on depth image was proposed for sleep posture recognition. In real sleep scenario, people usually sleep under a blanket or a quilt covering, and that is difficult for current methods of sleep posture recognition to classify sleep postures with the irregular layer. The proposal was designed to classify sleep postures using computer vision and machine learning method for applying



to a subject under covering. In preliminary stage, the depth image capturing an empty bed was transformed into world coordinate for calculating the bed plane. Each depth image capturing a subject was transformed into world coordinate, and the vertical distance of each depth pixel to the bed plane was calculated. From the input distance array of each depth image, the SVM method was adopted for classifying sleep postures into four classes: left side, right side, supine and stomach, in which left side and right side contained fetus, yearner and log types of sleep postures, supine contained soldier and starfish types of sleep postures, and stomach contained log and freefaller types of sleep postures. Experiments for simulating real sleep scenario with three conditions were carried out: without covering condition, blanket covering condition and quilt covering condition. Experimental results had high efficiency in left side and right side classification and normal results in supine and stomach classification, for the similarity between supine class and stomach class. In addition, there had a better performance in quilt covering condition than without covering condition and blanket covering condition, because the heavy layer enhances the features of sleep postures.

1.3 Organization of the Dissertation

The rest of this dissertation is structured as follows. In Chapter 2 the related works are discussed. In chapter 3 announces an unconstrained sleep browsing system for detecting and browsing sleep events. Chapter 4 presents a method of sleep posture recognition based on depth image for applying to a subject under covering. Finally, this dissertation is concluded and provides future directions in Chapter 5.



CHAPTER 2

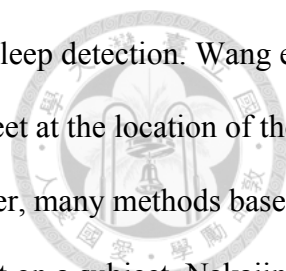
RELATED WORK

In the chapter, the context of the research in the backdrop of previous works is provided. Similar to the classification in the previous chapter, the related works of both constrained methods and unconstrained methods in sleep detection and sleep posture recognition are reviewed, and the advantages and limitations are addressed.

2.1 Constrained versus Unconstrained Sleep Detection

Since the late 1970s, numerous methods of sleep detection had been proposed for measuring a subject in bed. Normally, people shift their body positions within 40 to 60 per night, and many twitches occur in the sleep phase of rapid eye movement (REM) [9]. People with mood disorder, like busy mind with various thoughts, ideas and worries often have trouble sleeping, and unaware twitches also happen in a bad dream [10]. In addition, people with sleep disorder clearly have restless sleep.

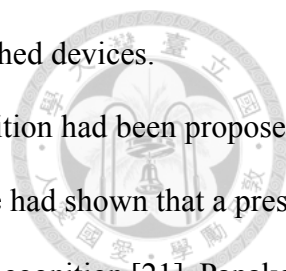
A growing number of sleep detection methods were proposed for measuring a subject in bed. According to device type, sleep detection methods can be classified into constrained and unconstrained methods. For reducing attached sensors, constrained methods used a ring with multiple sensors in sleep detection. According to the property of Electrodermal activity (EDA) with high frequency peaks in deep sleep stage, Akane used a ring with an electrode, a temperature sensor and an accelerometer to measure EDA, temperature and body movement for classifying sleep stages [11] [12]. In addition, Cole's algorithm was adopted to the motion data for sleep/wake identification [13]. The shortage of constrained method is the need of attached devices.



To address this, many studies had aimed to unconstrained method for sleep detection. Wang et al. designed a piezopolymer film (PVDF) sensor, which was placed under a sheet at the location of thorax to measure activities of respiratory movements and heartbeats [14]. Moreover, many methods based on image processing technique realized sleep measurement without any contact on a subject. Nakajima et al. used an IR camera and adopted optical flow method to visualize the velocity field of entire body, including respiration, cessation of breath, full posture change, limb movement and out of view [15]. Lee et al. used a depth camera, a temperature sensor and a humidity sensor for measuring sleep posture and room condition, presenting on a mobile application [16]. However, from the research on social science had shown that temperature cannot be considered as an objective parameter for sleep measurement, because a comfortable temperature for sleep differs individually [17]. Different from some of the works only measuring body movements, the goal of the study aimed to detect occurrences of sleep events in a sleep environment. A subject was considered as part of the sleep environment, and the body movements can be considered as one type of sleep event. In addition, all of the aforementioned methods only provided literal or graphical representations of sleep information. From the limited information, users were unable to know what exactly happened during sleeping. Hence, a sleep browsing system has been developed for detecting and browsing sleep events, and presented a sleep browsing interface with corresponding videos of sleep events.

2.2 Constrained versus Unconstrained Sleep Posture Recognition

Many studies had proposed constrained methods for sleep posture recognition. Heart sound had been used to detect sleep postures according to the changes of heart pressure [18]. One sensor was placed on the chest of a subject to measure heart sounds, and another sensor was implanted under the bed to detect body movements. SenseWear used an arm band to detect roll-over frequencies of body movements; however, it was unable to recognize accurate sleep posture only measuring one arm movement [19].



From the discussion, the shortage of constrained method is the need of attached devices.

To address this, many unconstrained methods for sleep posture recognition had been proposed. A pressure mattress was used for classifying sleep postures [20]. The evidence had shown that a pressure sensor with high spatial resolution has 92% high accuracy in sleep posture recognition [21]. Papakostas et al. considered the signals from the sensor array of a pressure mattress as a gray-scale image, and the Principal Component Analysis (PCA) method was adopted for reducing data dimension for SVM classification [22]. But the efficiency was highly depended on the body proportions of each subject. The commercial pressure mattress is not popular because of the price, especially a pressure mattress with high spatial resolution is expensive. Some methods of sleep posture recognition based on image processing technique had been proposed. Booranrom et al. used a depth camera to detect the arm angles for avoiding elders falling out of bed [23]. Lee et al. also used a depth camera to classify sleep postures into six classes, including fetus, log, yearner, soldier, freefaller and starfish [16]. However, both the aforementioned systems used the skeleton recognition of Microsoft Kinect SDK, and it has limitation with a subject under covering. Yu et al. proposed a method to classify postures into supine and lateral classes according to the relative position between head and shoulders [24]. It assumed that the chest position is lower than the head position in supine posture, and the shoulder position is higher than the head position in lateral posture. However, when a subject under heavy covering in left side or right side posture, the chest position with heavy layer was recognized as shoulder position and was misclassified into lateral category. Therefore, these methods are not practical in real sleep scenario. From the discussion, it also brings the main challenge of image-based method in sleep posture recognition. Hence, in the study, a method based on depth image was proposed to realize the sleep posture recognition in the condition of a subject under covering.

2.3 Summary

The brief descriptions, advantages and deficiencies of the related works have been provided. A brief description of solutions to the above mentioned problems are listed as follows. Unlike current methods only providing literal or graphical representations, a sleep browsing system has been developed for detecting and browsing sleep events. For the efficiency of the sleep browsing system, epoch method was proposed to record sleep events, instead of whole night recording. A browsing interface with sleep diagram was provided for examining sleep by playing corresponding videos of sleep events. Furthermore, for solving the problem of a subject under covering, a method of sleep posture recognition based on depth image was proposed for applying to a subject under covering. In the following chapter, the details of the epoch method for recording sleep event, and a method of sleep posture recognition based on depth image are presented.



CHAPTER 3

SLEEP BROWSING SYSTEM FOR SLEEP EVENT

DETECTION AND BROWSING

3.1 Sleep Event Type

Ideal sleep consists of falling asleep quickly, overnight sleep and refreshed experience of waking up; however, sleep is interrupted in some cases [10] [25]. After poor sleep, people may have difficulty to concentrate on daily activities, and it is also harm to health for the suppression effect on immune system [26] [27]. To better understand the optimal sleep condition, some researches on social science indicated that darkness and tranquility are basic conditions for sleep [28]. Usually, people may have difficulty to fall asleep in a light environment. In addition, noise problems such as sources of noises from outside traffic, or talking on a street result in poor sleep condition. The sources of noises are also caused by a sleep partner with different sleep schedule, for example reading, or typing on a computer in the sleeping room [17]. Especially, a snoring partner seriously affects sleep experiences of others [29]. Considering other conditions, a comfortable temperature for sleep differs individually [17]. In addition, a bed with suitable firmness is helpful for sleep, but it also differs by different shapes and sizes of people [30]. Hence, only lighting and sound conditions were considered in the study. In addition, a subject in bed was considered as part of the sleep environment, and body movements of the subject was considered as one type of sleep event. In the study, sleep events were classified into three types: motion event, lighting event and sound event.

3.2 System Overview

In the section, system overview of the sleep browsing system is described. A device (Kinect for Windows) with a depth camera, a color camera and a microphone was used to detect three types of sleep events showing on Figure 3.1, with 8-bit VGA resolution (640×480 pixels) of color image, 11-bit VGA resolution (640×480 pixels) of depth image, and 24-bit resolution of audio signal. Frame rate of depth image and color image is 30 Hz, and sampling rate of audio signal is 16 kHz.

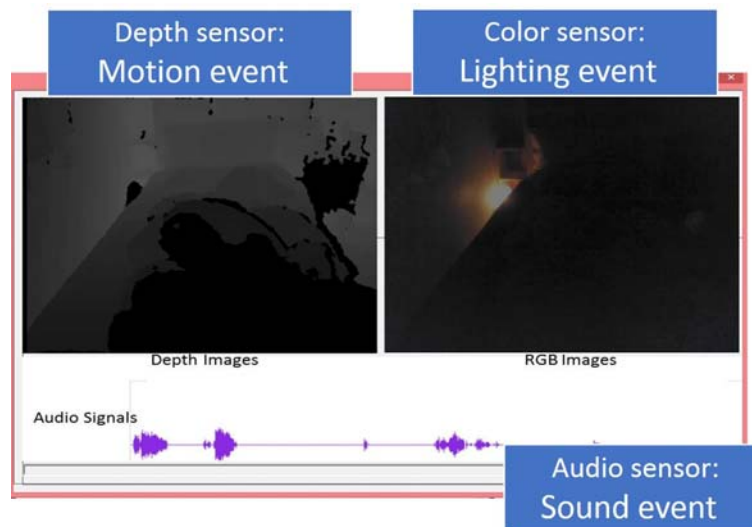


Figure 3.1: Relationship between sensor and sleep event.

3.2.1 System Setup

For reducing noises, a region of interest (ROI, 320×350 pixels) was selected for covering the bed region in sleep detection. In Figure 3.2, the device was set at the distance of 0.2 meters and in the height

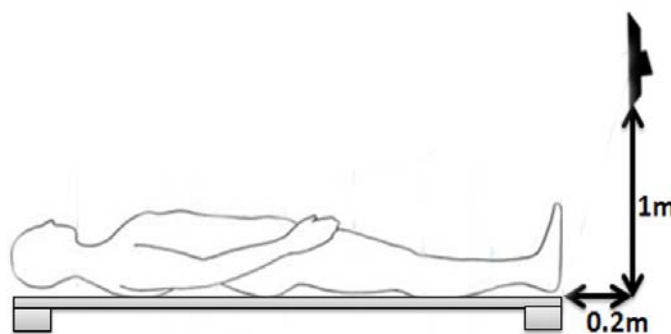
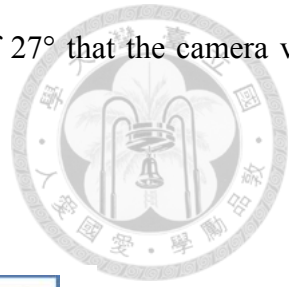


Figure 3.2: An illustration of device setting.

above the bed of 1 meter. It set in front of a bed at a depression angle of 27° that the camera view covered the entire body of a subject.



3.2.2 System Flow

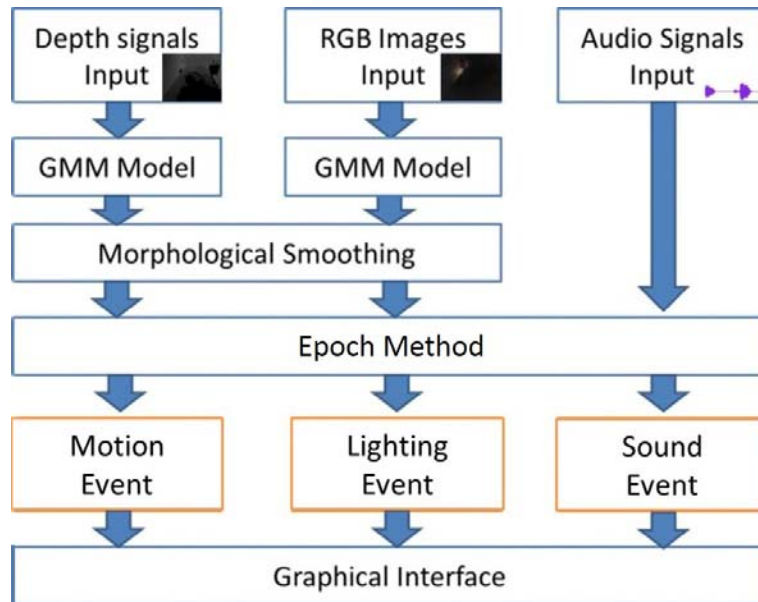


Figure 3.3: Flow chart of sleep browsing system.

Flow chart of the sleep browsing system is showing on Figure 3.3. From the input of depth image stream and the input of color image stream, GMM background modeling was used to measure body movements of a subject in bed and lighting changes in a sleep environment. For reducing noises, the results of foreground segmentation were processed by morphological smoothing. According to sensor type, sleep events were classified into three types: motion event, lighting event and sound event. Epoch method was applied to record sleep events, in which depth images, color images and audio files were recorded simultaneously. Finally, a browsing interface with sleep diagram was provided for browsing sleep events, presenting the score curves of sleep events and integrated videos.

3.3 Sleep Event Detection and Recording

In the section, steps of sleep event detection and recording in the sleep browsing system are introduced, followed by background modeling for measuring body movements and lighting changes, the proposed

epoch method for recording sleep events continuously, and a browsing interface with sleep diagram for browsing sleep events.



3.3.1 Background Modeling

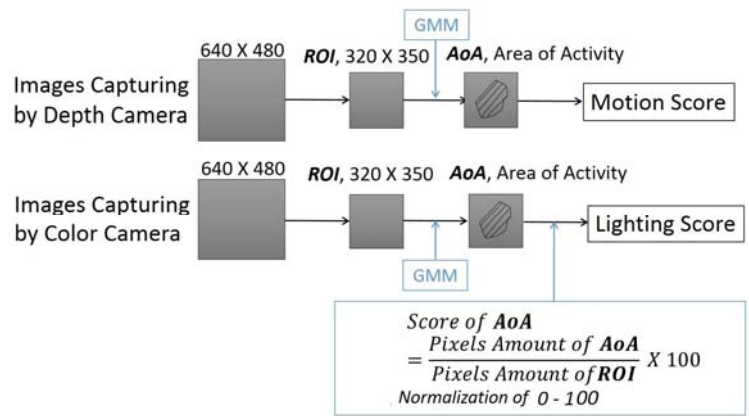
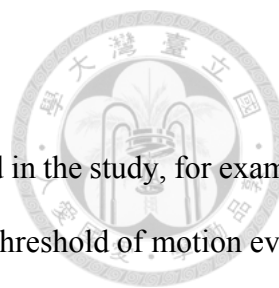


Figure 3.4: Background modeling for measuring body movements and lighting changes.

The problem of measuring body movements of a subject in bed can be regarded as foreground detection. Because the raw data of depth image has the problem of missing bits and flickering issues from multiple reflections, transparent objects or scattering surfaces, and background subtraction method is not an appropriate solution for the high variety condition. Hence, GMM background modeling was adopted in the study for measuring body movements and lighting changes showing on Figure 3.4 [31]. From the input of depth image stream, GMM background modeling was applied to the ROI region of depth images for measuring body movements. In addition, the problem of measuring lighting changes in a sleep environment can be also regarded as foreground detection. From the input of color image stream, GMM background modeling was applied to the ROI region of color images for measuring lighting changes. Area of activity (AoA) is percentage of foreground segmentation area to the ROI area of an image. From the AoA score of a depth image and AoA score of a color image, motion score and lighting score were calculated, respectively. Both scores were normalized to the same scale (0-100). In the study, motion score was considered as body movements, and lighting score was considered as lighting changes.



3.3.2 Empirical Threshold of Sleep Event

Motion event was defined including any body movements of a subject in bed in the study, for example turning behaviors, or crawling into bed and out of bed. For determining the threshold of motion event, in preliminary stage, a turning behavior from right side to left side was recorded with corresponding depth images and results of foreground segmentation. After calculating motion scores of the turning behavior, empirical threshold of motion event was determined (10, scale: 0-100).

Lighting event was defined including any lighting changes in the sleep environment in the study, for example turning on/off a light, or sunlight from outside of the window. For the property of GMM background modeling, lighting score is only considered as lighting changes in a dark environment. In a light room without lighting changes from outside of the room, the lighting score has the same meaning as motion score that the changes of score value are caused by body movements. In preliminary stage, the sleep browsing system was tested in a light room with curtains, and recorded a turning behavior. By observing the recording of motion scores and lighting scores of the turning behavior, the difference between motion score and lighting score is less than 1. On the contrary, if the difference is greater than 1, the lighting score can be regarded as lighting changes. A rescoring rule was proposed for correcting lighting score in the circumstance.

$$\text{if } |\text{motion score} - \text{lighting score}| < 1, \text{ lighting score} = 0 \quad (1)$$

If the difference is less than 1, the lighting score has the same meaning as motion score, and the lighting score is rescored to 0. Figure 3.5 shows an example of applying the rescoring rule. Before rescoring, the number of lighting events is similar to the number of motion events showing on the top graph of Figure 3.5. After rescoring, the number of lighting events is rapidly decreasing showing on the bottom graph of Figure 3.5. Therefore, the rescoring rule was applied to correct the errors of sleep event

detection in the daytime. Empirical threshold of lighting event was set equal to empirical threshold of motion event by default (10, scale 0-100).

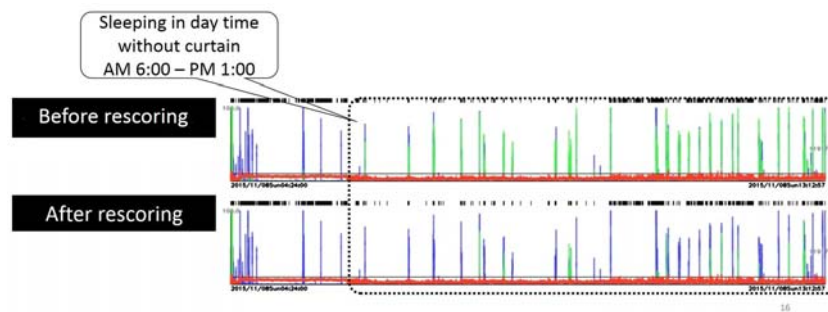


Figure 3.5: Rescoring rule for correcting lighting score (Blue: motion event, green: lighting event and red: sound event).

Sound event was defined including any sounds at volume over 60 decibels in the study, for example normal conversation. These sounds may rouse people from sleeping. For determining the threshold of sound event, a sound test of normal conversation was recorded in preliminary stage. The sound score was also normalized to the same scale of motion score and lighting score, and empirical threshold of sound event was determined from the recording of sound scores (40, scale 0-100).

3.3.3 Motion Threshold Adjustment

The threshold of motion event is highly depended on the position of device setting, because the motion score is calculated according to the percentage of foreground segmentation area to the ROI area of a depth image. The device was set in a fix position showing on Figure 3.2; however, body movements of a subject are greater or less than normal level in some cases for different sizes of bodies. In addition, the severity of lighting effect and noise problem is also different in diverse sleep environments. For improving reliability of the sleep browsing system, the function of adjusting threshold was provided.

Figure 3.6 shows detection interface of the sleep browsing system. The bars on the top of the interface allow users to adjust threshold of each sleep event. Sometimes, users may have difficulty to determine an appropriate threshold of motion event, and the auto adjustment function allows users to

reset the threshold automatically. After clicking the auto adjustment button, the sleep browsing system plays a guiding voice to direct users lying on the bed, and then turning to left side or right side every 20 seconds within 1 minute. After the guiding, the recording of motion scores is arranged in decreasing order, and reset the original threshold of motion event to the max motion score showing on the detection interface. Before sleep, users start the sleep browsing system to detect and record sleep events by clicking the start button, and finish the recording by clicking the exit button after waking up.

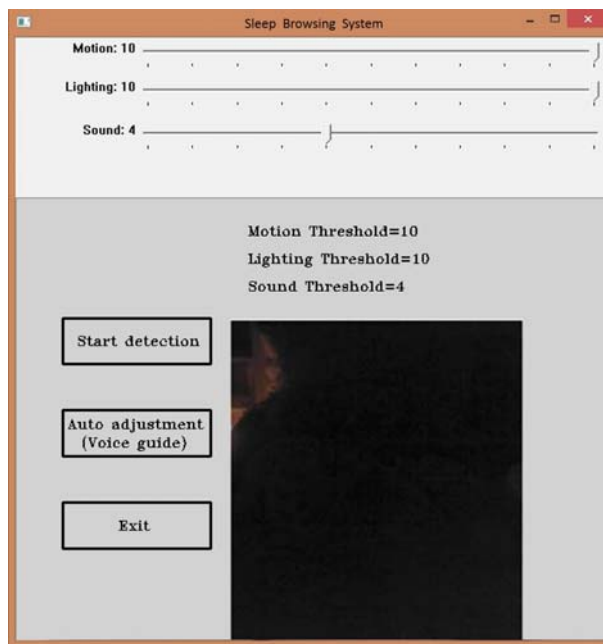


Figure 3.6: Detection interface of sleep browsing system.

3.3.4 Epoch Method

For recording sleep events continuously, epoch method was proposed in which calculates data iteratively at a constant interval in a model of the form:

$$\left\{ \begin{array}{l} \text{if } A_0 = \text{true}, \text{start recording of an event} \\ \text{if } A_1 = \text{true}, \text{recording of the event continues} \\ \quad ; \text{ otherwise, end recording of the event} \end{array} \right. \quad (2)$$

where A_0 , A_1 = activity count of the current epoch and the following epoch, respectively. In preliminary stage, empirical threshold of each sleep event was determined. Using epoch length of 3 seconds, the equation was applied to calculate score of each epoch iteratively for recording sleep events. If score of the current epoch is greater than empirical threshold, an event is detected and the system starts recording of the event. If score of the following epoch is greater than empirical threshold, the system continues recording of the event; otherwise the system ends recording of the event. In the study, the equation was applied to motion score, lighting score and sound score.

Figure 3.7 shows the steps of epoch method. Given motion score set S_m , lighting score set S_l and sound score set S_s , initial bool states of motion event B_m , lighting event B_l and sound event B_s are set false which define detection of sleep events. Using epoch length of 3 seconds, a timer is set to record sleep events continuously, in which a buffer is set to capture data including depth images, color images and audio files. In addition, the buffer captures data of 1 epoch continuously. Therefore, the buffer captures data before event happening, and that is helpful for examining sleep. By the definition of equation (2), if motion score of current epoch S_{m0} is greater than empirical threshold T_m within 3 seconds, the bool state of motion event B_m is set true, and the system starts recording of the motion event. Once recording of an event is started, the buffer data is recorded every 3 seconds at least repeating 4 times, and motion event set E_m , lighting event set E_l and sound event set E_s are updated. The minimum length of an event consists data of 4 epochs (12 sec.). The equation is also applied to lighting score and sound score for recording lighting event and sound event. During the recording, once an event was detected in the following epoch, the bool state of the event is set true, and the system continues recording of the event every 3 seconds at least repeating 4 times. Otherwise, the system ends recording of the event, bool states B_m , B_l , and B_s are reset to initial state, buffer data is released, and timer is reset. The steps of (2) to (4) are repeated every 3 seconds in the method.



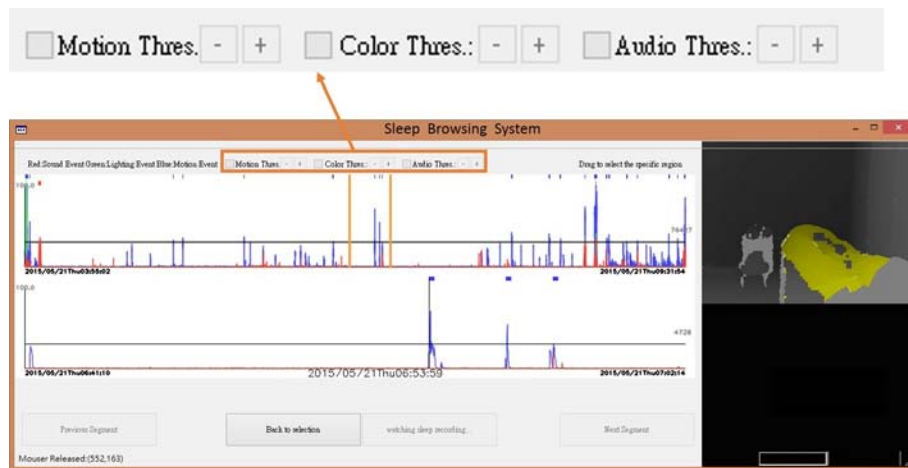
```
1. Input:
2.     Given motion score set  $S_m$ , lighting score set  $S_l$  and sound score set  $S_s$ ;
3. Output:
4.     Motion event set  $E_m$ , lighting event set  $E_l$  and sound event set  $E_s$ ;
5.     (1)  $B_m, B_l, B_s = \text{false}$ ;
6.     (2) do
7.         if( $S_{m0} > T_m$ )
8.              $B_m = \text{true}$ ;
9.         else if( $S_{l0} > T_l$ )
10.             $B_l = \text{true}$ ;
11.        else if( $S_{s0} > T_s$ )
12.             $B_s = \text{true}$ ;
13.        end if
14.
15.        Capture buffer data;
16.        while (time  $\leq$  3sec.)
17.    (3) if ( $B_m = \text{true} \parallel B_l = \text{true} \parallel B_s = \text{true}$ )
18.        start recording;
19.
20.        if (start recording)
21.            Do
22.                update  $E_m, E_l$  and  $E_s$ ;
23.                while (repeat  $\leq$  4);
24.            end if
25.        end if
26.    (4)  $B_m, B_l, B_s = \text{false}$ ;
27.        release buffer data;
28.        reset timer;
29.    (5) repeat (2) to (4);
```

Figure 3.7: Epoch method.

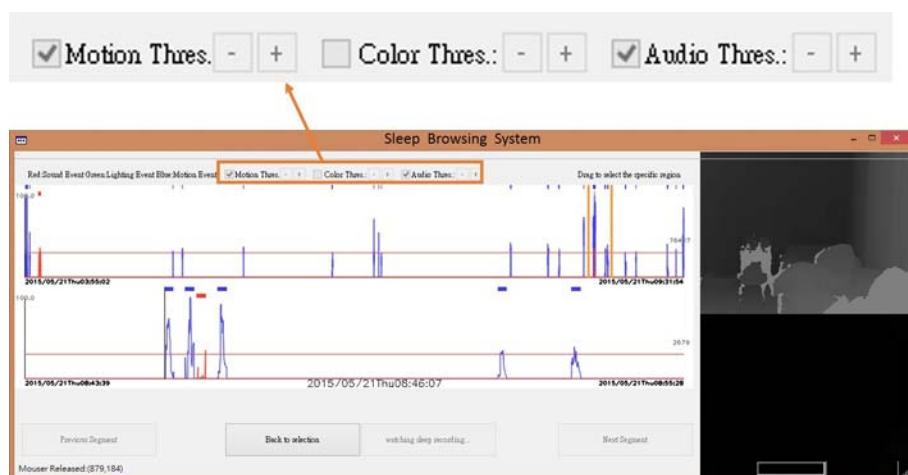
3.3.5 Sleep Diagram for Browsing Sleep Events

A browsing interface with sleep diagram was provided for browsing sleep events showing on Figure 3.8 (a). Blue color, green color and red color represent the score curves of motion event, lighting event and sound event, respectively. The marks on the top of sleep diagram indicate the timestamp of sleep events according to the representing colors. Empirical threshold of each sleep event was normalized to the same value as the default threshold of three types of sleep events, representing in black horizontal

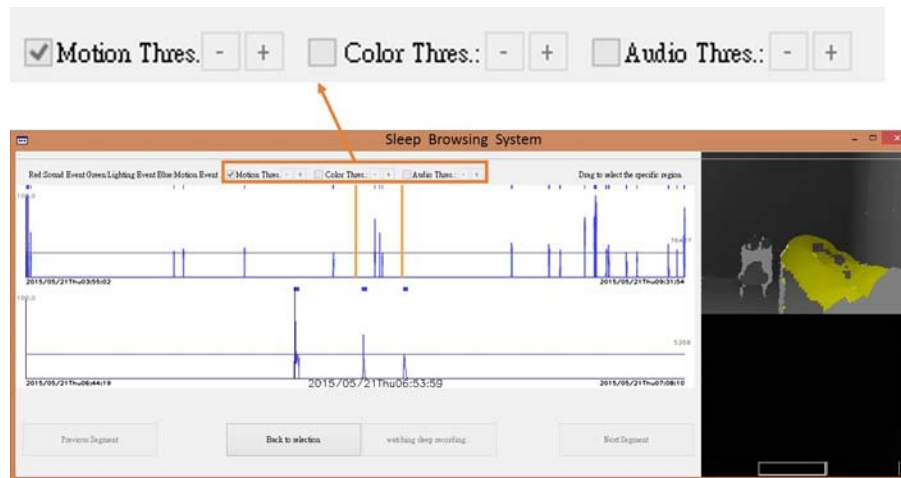
line on the sleep diagram. In addition, the buttons of previous segment and next segment are helpful for users to browse sleep of different days. In Figure 3.8 (b) and (c), checkbox on the top of the browsing interface allows users to browse and adjust threshold of each sleep event independently. When threshold is changed, color horizontal line represents threshold of each sleep event according to the representing colors showing on Figure 3.8 (d). The function of adjusting threshold is helpful for examining sleep that high threshold makes significant sleep events standing out; on the contrary, low threshold reveals details of sleep events. Users select an interested region on the sleep diagram, the selected region is expanded, and the corresponding videos of sleep events in the region is playing.



(a)



(b)



(c)



(d)

Figure 3.8: Browsing interface of sleep browsing system: (a) Default threshold of each sleep event representing in black horizontal line, (b) and (c) Checkbox on the top for browsing and adjusting threshold of each sleep event independently, (d) Threshold of each sleep event representing in color horizontal line (Blue: motion event, green: lighting event and red: sound event).

3.4 Experiments on Overnight Sleep

In the section, performance of the sleep browsing system is evaluated in overnight sleep experiments. Sleep/wake identification method is introduced for sleep quality evaluation. Finally, sleep events from diverse sleep environments, and the correlation between sleep event and sleep quality is discussed.



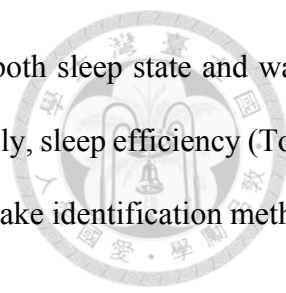
3.4.1 Sleep/Wake Identification

Table 3.1: Comparison of sleep/wake identification algorithms.

Sleep/Wake Identification	Year	Wrist activity	Epoch length	Scoring interval	Rescoring rule	Accuracy
Webster [33]	1982	Dominant hand	2 sec.	1 min.	5	94.46%-94.74%
Cole [13]	1992	Non-dominant hand	2 sec.	1 min.	5 (Same as Webster)	87.93%-88.25%
Sadeh [34]	1994	Dominant hand Non-dominant hand	30 sec.	1 min.	1	91.37%-92.77%

For evaluating experimental results, sleep/wake identification method was adopted in the study for sleep quality evaluation. A historical activity-based method, actigraph, was proposed by Tryon [32]. Based on actigraph method, actigraphy is a wearable device with an accelerometer and a lighting sensor for measuring activities of a subject in bed. In clinical therapy, actigraphy is worn on the wrist of dominant hand or non-dominant hand for comparing with PSG data epoch-by-epoch. Three major algorithms of sleep/wake identification are listed on Table 3.1 [13] [33] [34]. The accuracy of Webster's algorithm was determined by comparing sleep/wake scores with Electroencephalography (EEG) data, and the accuracy of Cole and Sadeh's algorithms agreed sleep/wake scores with PSG data. The evidence had shown in the evaluation of total sleep time in long-term period, and there is a correlation of 0.81 between actigraphy measurement and PSG measurement [35]. Hence, total sleep time can be calculated by activity data. In addition, Sadeh's algorithm had been evaluated by adding a constant value or multiplying a constant ratio to the activity value of each epoch, and only resulted in 0.4% to 1.4% changes in agreement rates between PSG and actigraphy data, and in 1.5% to 3.6% change in sleep efficiency calculating by actigraphy data [34]. Hence, in the study, Sadeh's algorithm was adopted for sleep quality evaluation using the device with different sampling rate.

From the input of motion score set, sleep/wake scores were calculated by Sadeh's algorithm using epoch length of 30 seconds, by considering the activity count of each epoch during the current epoch, the preceding 5 epochs and the following 5 epochs. For improving performance of the algorithm, the sleep/wake scores were rescored to 1-minute interval by the rescoring rule of Sadeh's



algorithm. For example, there is a high possibility of wakefulness when both sleep state and wake state exit in the same minute, and the minute is rescored as wake state. Finally, sleep efficiency (Total sleep time/total time in bed) can be calculated. Hence, in the study, sleep/wake identification method was applied to calculate total sleep time for sleep quality evaluation.

3.4.2 Experiments on Discovering Sleep Events

Table 3.2: Sleep parameters of overnight sleep experiments.

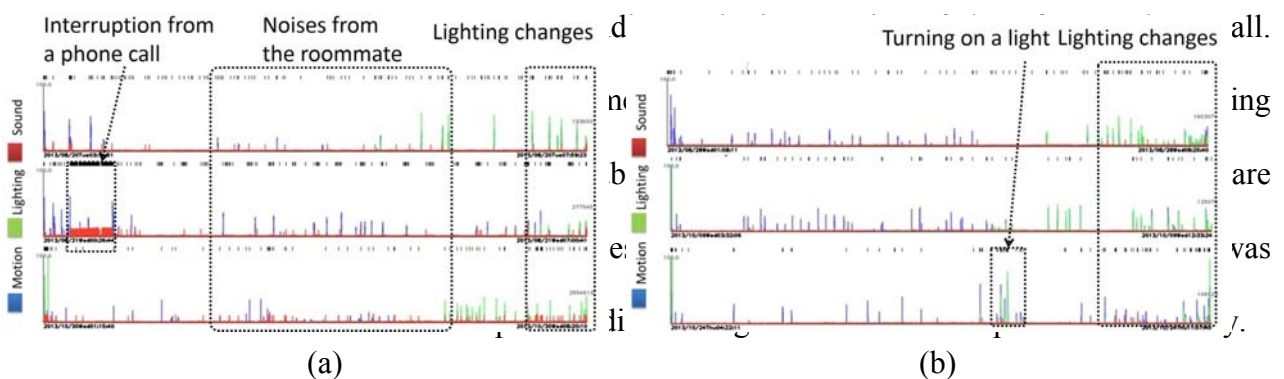
Subject	TST (min.)	TTB (min.)	SE (%)	Motion event (%)	Lighting event (%)	Sound event (%)
A	361±55	371±54	96.97±1.54	0.48±0.23	0.23±0.16	0.15±0.23
B	372±86	396±93	93.91±0.44	0.28±0.18	0.05±0.05	0.06±0.05
C	396±48	436±47	90.67±2.46	0.59±0.18	0.06±0.04	0.66±0.32
D	430±84	444±79	96.53±2.28	0.66±0.11	0.06±0.02	0.16±0.18
E	329±68	349±64	93.92±2.48	0.30±0.32	0.04±0.01	0.00±0.00
Average	381±74	405±76	94.04±3.17	0.60±0.28	0.14±0.15	0.26±0.34

*TST: total sleep time, TTB: total time in bed, SE: sleep efficiency.

For discovering sleep events in diverse sleep environments, space of the experiments was set in home scenario, and it also avoided the effect of an unfamiliar environment which may result in trouble sleeping. For unchanging sleeping habits of participants, all participants went to bed as usual and allowed to turn on a small lamp during sleeping. In addition, for comparing the recording of sleep events from diverse sleep environments, all participants were not allowed to change the default threshold of each sleep event in sleep detection. Our samples of 5 subjects included 4 men and 1 woman, ranging in age between 31 and 39 years (Mean = 34.2, SD = 3.19). The experiments recorded 25 nights (1 participant: 7 nights, 2 participants: 5 nights and 2 participants: 4 nights). In addition, the extreme value of zero sleep efficiency which recorded a sleepless night of participant E was eliminated. For protecting privacy of participants, the recording of videos of sleep events was only watched by themselves. After the experiments, all participants were interviewed to describe the sources of sleep events.

Sleep parameters of the overnight sleep experiments are listed on Table 3.2. Figure 3.9 shows

sleep diagrams of each participant. Firstly, the recording of motion events is discussed. Normally, people shift their body positions within 40 to 60 per night [9]. In Figure 3.9, there are frequent motion events in the recording of all participants. In Table 3.2, the number of motion events of participant C and participant D is slightly higher than the others. Especially, motion events in the beginning of sleep showing on Figure 3.9 (e) recorded a bad sleeping habit for the participant was not preparing for sleep. The recording of lighting events is further discussed. In Table 3.2, the number of lighting events of participant A is obvious higher than the others. In Figure 3.9 (a) and (b), both participants A and participant B recorded lighting events. Because they did not use curtains in the sleeping room, and sunlight from outside of the window were recorded. The occurrence of lighting event showing on the third graph of Figure 3.9 (b), indicates the interruption of sleep from turning on a light. Finally, the recording of sound events is discussed. In Table 3.2, the number of sound events of participant C is obvious higher than the others. Both participant C and participant D had serious noise problems. In Figure 3.9 (c), the sources of noises were from the outside traffic where Participant C lived near major road of the city. The noise problem of participant D was caused by the pumping sounds from the basement, and that explains the regular sound events showing on Figure 3.9 (d). In Figure 3.9 (a), the sources of noises were caused by the roommate of participant A. In addition, the second graph of



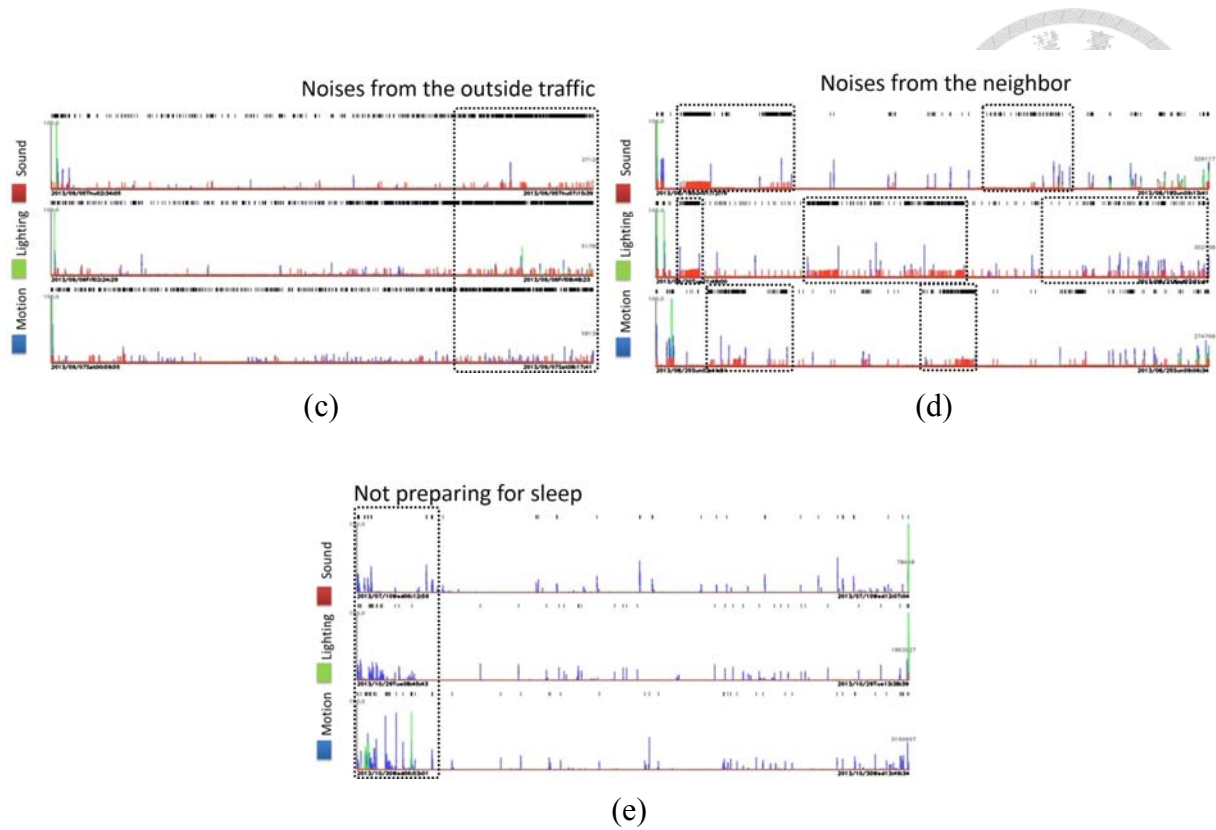
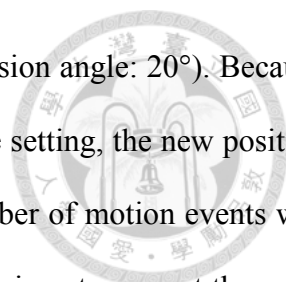


Figure 3.9: Samples of sleep diagrams: (a) Participant A, (b) Participant B, (c) Participant C, (d) Participant D and (e) Participant E (Blue: motion event, green: lighting event and red: sound event).

3.4.3 Experiments on Sleep Quality Evaluation

For evaluating the correlation between sleep event and sleep quality, the overnight sleep experiments for two weeks were carried out. In the stage of subject screening, according to the statistics of Pre-Sleep Arousal Scale (PSAS) score in cognitive part (Normal: mean = 13.11, SD = 4.18; insomnia: mean = 23.58, SD = 7.07), the subjects with moderate insomnia which was caused by poor mental state were selected (PSAS > 23, mean = 29.56, SD = 3.39) [36]. The subjects had poor sleep experiences which increase the possibility of sleep events in their sleep environments, and that is helpful for evaluating the correlation between sleep event and sleep quality. The samples of 18 subjects included 10 men and 8 women, ranging in age between 19 to 25 years (Mean = 21.39, SD = 1.6). In addition, the device was set in a closer position than the previous experiments for the



limitation in space of participants (Distance: 50 cm, height: 55 cm, depression angle: 20°). Because the threshold of motion event is highly depended on the position of device setting, the new position of device setting was tested by recording an overnight sleep, and the number of motion events was not notable increases. Therefore, the threshold of motion event in the experiments was set the same as the previous experiments, and the rest setting of the experiments was the same as the previous experiments. The experiments recorded 250 nights and assumed that each participant recorded 14 nights; however, 3 participants missed 1-night recording, and 1 participant recorded 15 nights.

Sleep parameters of the overnight sleep experiments are listed on Table 3.3. Firstly, the correlation between motion event and sleep quality is discussed. A hypothesis was assumed in the experiments that high motion behavior has negative effects on sleep quality. In Table 3.3, there are high negative correlations between motion event and sleep efficiency in the recording of 8 participants (44%: participants A, D, G, H, L, M, N and P), and moderate negative correlations between motion event and sleep efficiency in the recording of 6 participants (33%: participants B, F, G, K, Q and R). Normally, people shift their body positions within 40 to 60 per night [9]. If the frequency of turning behavior exceeds the normal level, it results in poor sleep experience. The participants with insomnia which was caused by poor mental state increase body movements during sleeping, and there are negative correlations between motion event and sleep efficiency in the recording of most participants. Hence, the hypothesis has been proved that high motion behavior has negative effects on sleep quality.

Sleep efficiency is highly depended on distribution of motion event, because total sleep time is calculated by sleep/wake identification algorithm, considering the activity count of the current epoch, the preceding 5 epochs and the following 5 epochs. For example, the number of motion events in the recording of participant G is similar to participant I's; however, motion events had strong effects on sleep efficiency of participant G, but few effects on sleep efficiency of participant I. An example of relationship between distribution of motion event and sleep efficiency is showing on

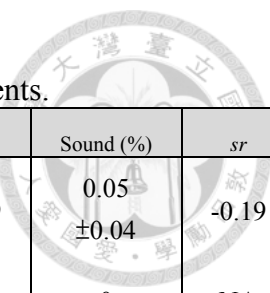


Table 3.3: Sleep parameters of overnight sleep experiments.

Subject	TST (min.)	TTB (min.)	SE (%)	Motion (%)	<i>mr</i>	Lighting (%)	<i>lr</i>	Sound (%)	<i>sr</i>
A	396.6 ±46.18	410.79 ±42.78	96.42 ±2.98	1.02 ±0.19	-0.85**	0.03 ±0.07	-0.19	0.05 ±0.04	-0.19
B	440.64 ±54.78	456.57 ±58.58	96.58 ±1	1.53 ±0.24	-0.69*	0.07 ±0.14	-0.1	0	NA
C	432.38 ±54.18	444.38 ±55.01	97.29 ±0.83	1.19 ±0.13	-0.19	1.19 ±0.13	-0.19	0	NA
D	384.57 ±57.71	400.79 ±49.6	96.06 ±2.87	1.42 ±0.38	-0.77**	0.02 ±0.04	-0.16	0	NA
E	283.21 ±71.29	299.29 ±73.16	94.32 ±2.09	1.46 ±0.44	-0.49	0.35 ±0.08	-0.11	0.06 ±0.04	-0.01
F	317.43 ±68.04	341.86 ±70.89	92.76 ±2.09	1.61 ±0.3	-0.55*	0.11 ±0.1	0.18	0	NA
G	410.21 ±81.94	428.07 ±85.79	95.84 ±1.51	1.21 ±0.32	-0.89**	0.06 ±0.06	0.06	0	NA
H	297.43 ±35.14	312.26 ±36.69	95.11 ±2.19	1.84 ±0.37	-0.92**	0.05 ±0.09	0.3	0	NA
I	377.64 ±36.71	390.5 ±36.52	96.11 ±2.32	1.21 ±0.3	-0.24	0.04 ±0.04	0.02	0	NA
J	317.43 ±57.78	330.29 ±58.07	96.05 ±1.1	1.39 ±0.26	-0.53*	0.05 ±0.04	-0.29	0	NA
K	377.31 ±158.91	397.77 ±164.23	94.36 ±1.47	1.88 ±0.32	-0.54*	0.16 ±0.07	-0.35	0.12 ±0.06	-0.35
L	442.29 ±51.21	487.86 ±67.27	90.96 ±3.33	2.47 ±0.35	-0.85**	0.16 ±0.14	-0.69*	0.47 ±0.24	-0.55*
M	381 ±68.54	404.57 ±75.73	94.37 ±2.69	1.17 ±0.31	-0.87**	0.1 ±0.1	-0.3	0 ±0	-0.12
N	486.53 ±67.2	503.87 ±69.75	96.59 ±1.86	1.51 ±0.29	-0.78**	0.01 ±0.01	-0.36	0	NA
O	397.57 ±18.58	405.07 ±19.02	98.15 ±0.4	0.52 ±0.1	-0.46	0.01 ±0	NA	0.01 ±0.01	-0.05
P	388.85 ±60.95	425.31 ±68.17	91.52 ±3.35	2.18 ±0.37	-0.81**	0.18 ±0.12	0.29	0 ±0.01	0.05
Q	412.38 ±50.82	435 ±55.98	94.87 ±1.73	1.85 ±0.19	-0.67*	0.08 ±0.03	-0.6*	0	NA
R	386.57 ±44.75	418.14 ±48.12	92.49 ±3.01	1.6 ±0.43	-0.64*	0.41 ±0.26	0.56*	0.11 ±0.15	0.03

*TST: total sleep time, TTB: total time in bed, SE: sleep efficiency; *mr*, *lr* and *sr* represent the correlation coefficient between sleep efficiency and motion event, lighting event and sound event, respectively.

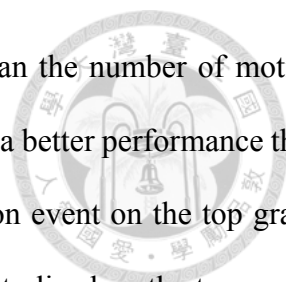


Figure 3.10. The number of motion events on the top graph is greater than the number of motion events on the bottom graph. However, sleep efficiency of the top graph has a better performance than sleep efficiency of the bottom graph. Comparing the distribution of motion event on the top graph with that of the bottom graph, the distribution of motion event is more centralized on the top graph. In the central distribution of motion event, segments without activities are classified into sleep category by sleep/wake identification algorithm, and improves the performance of sleep efficiency. On the contrary, although the number of motion events on the top graph is less than that of the bottom graph, segments with activities are classified into wake category in the sparse distribution of motion event, and also affects the performance of sleep efficiency. Hence, the effect of motion event on sleep quality differs individually, considering both quantity and distribution of motion event.

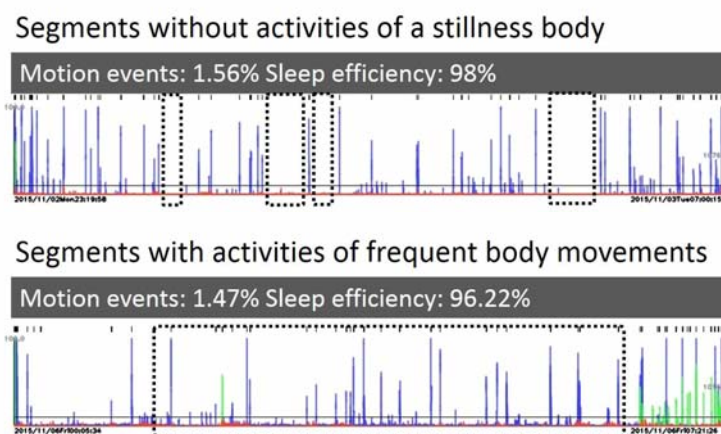


Figure 3.10: Distribution of motion event (Blue: motion event, green: lighting event and red: sound event).

The correlation of lighting event and sleep quality is further discussed. In Table 3.3, there are moderate negative correlations between lighting event and sleep efficiency in the recording of participant L and participant Q, and moderate positive correlations between lighting event and sleep efficiency in the recording of participant R. In Figure 3.11 (b) and (c), both participant Q and participant R recorded lighting events at the end of sleep which were caused by sunlight from outside of the window. However, the positive correlation in the recording of participant R indicates that

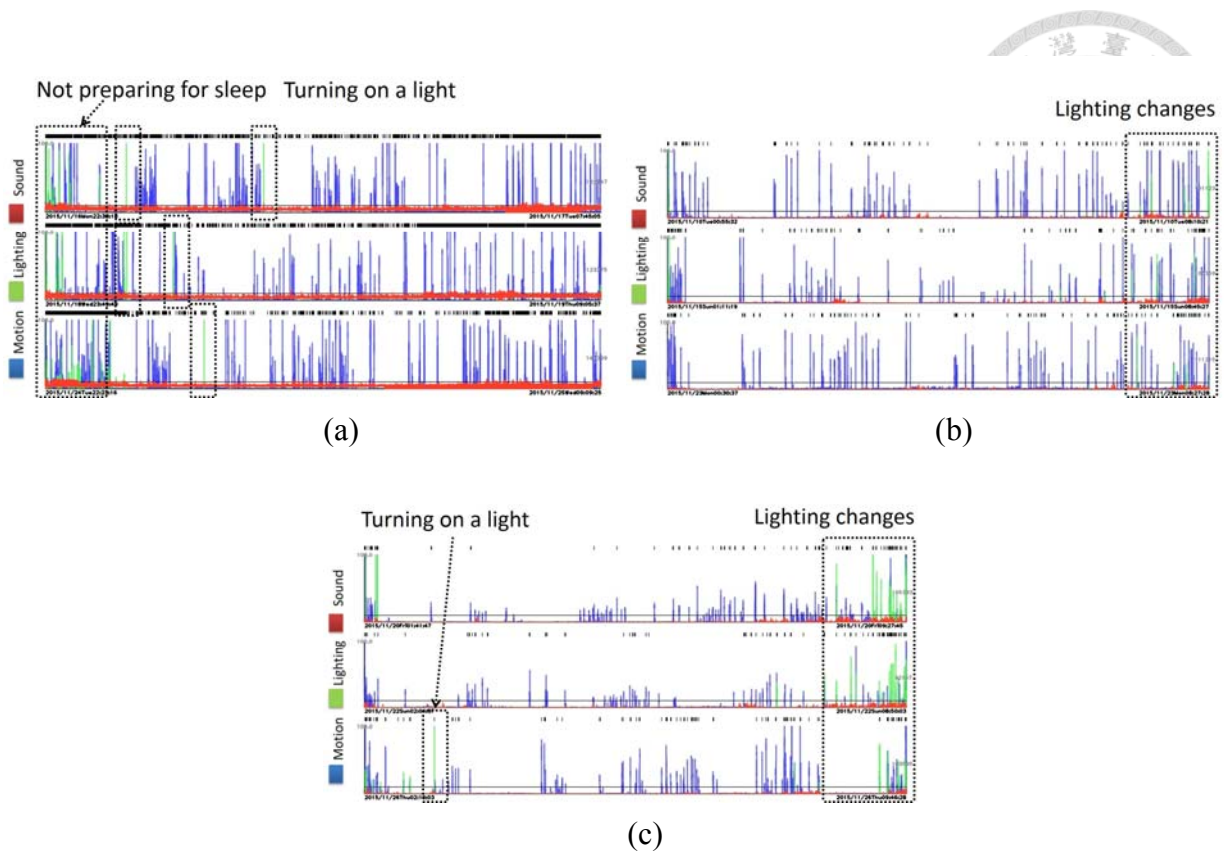
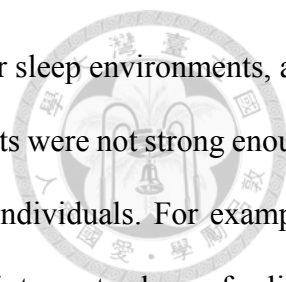


Figure 3.11: Samples of sleep diagrams: (a) Participant L, (b) Participant Q and (c) Participant R (Blue: motion event, green: lighting event and red: sound event).

tolerance to light varies with different individuals. For example, some participants were sleeping in a darkness room, but the others were used to sleep with a small lamp. In addition, lighting events in the middle of sleep recorded the interruption of sleep from turning on a light showing on Figure 3.11 (a), and lighting events at the beginning of sleep also recorded a bad sleeping habit of participant L, for the participant was not preparing for sleep. Most participants recorded few lighting events during sleeping, and the correlations between lighting event and sleep quality of these participants were not strong enough for discussion. Hence, the effect of lighting event on sleep quality differs individually, for tolerance to light varies with different individuals.

Finally, the correlation of sound event and sleep quality is discussed. In Table 3.3, there is moderate negative correlation between sound event and sleep efficiency in the recording of participant L. In Figure 3.11 (a), the score curve of sound event is obvious on the sleep diagrams, and the sources of noises were caused by the hamming sounds of ambulances, because of the participant



lived near a hospital. Most participants did not have noise problems in their sleep environments, and the correlations between lighting event and sleep quality of these participants were not strong enough for discussion. In addition, tolerance to noise also varies with different individuals. For example, noises may not rouse participants when they are in deep sleep, but may interrupt sleep of a light sleeper. Hence, the effect of sound event on sleep quality differs individually, for tolerance to noise varies with different individuals.

3.5 Summary

Unlike other approaches only measured activities of a subject in bed, the sleep browsing system has been developed for detecting and browsing sleep events in diverse sleep environments. Both activities of a subject in bed and the environmental effects were considered, and the epoch method was provided for recording sleep events continuously. A sleep browsing interface with score curves and integrated videos of sleep events was provided for browsing sleep. Finally, the overnight sleep experiments were carried out, and the experimental results showed the efficiency and reliability of the sleep browsing system.



CHAPTER 4

SLEEP POSTURE RECOGNITION BASED ON DEPTH IMAGE

4.1 Sleep Posture Type

Common sleep postures include fetus, yearner, soldier, starfish, supine and stomach postures showing on Figure 4.1. In the study, sleep postures were classified into four classes: left side, right side, supine and stomach, in which left side and right side contained fetus, yearner and log types of sleep postures, supine contained soldier and starfish types of sleep postures, and stomach contained log and freefaller types of sleep postures.

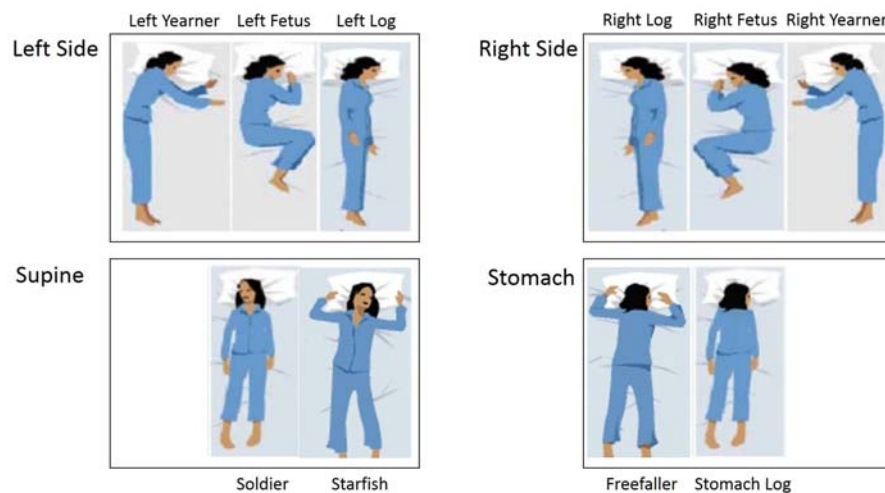


Figure 4.1: Sleep posture type.

4.2 Sleep Posture Recognition

Steps of sleep posture recognition are showing on Figure 4.2. Firstly, projective coordinate system of each depth image was transformed into world coordinate system, representing with 3D point cloud.

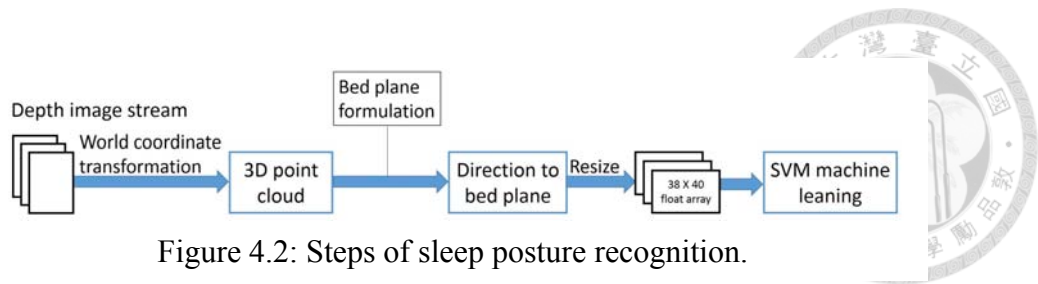


Figure 4.2: Steps of sleep posture recognition.

Figure 4.3 (a) shows a depth image capturing an empty bed. In preliminary stage, ROI region of the depth image was selected showing on Figure 4.3 (b), and was transformed into world coordinate for calculating the bed plane showing on Figure 4.3 (c). Figure 4.3 (a) shows a depth image capturing a subject. In Figure 4.3 (e), ROI region of the depth image was selected, and was transformed into world coordinate showing on Figure 4.3 (f). The vertical distance of each depth pixel to the bed plane was calculated. From the input distance array of each depth image (Resolution: 304×320), the array was resized for SVM classification (Resolution: 38×40).

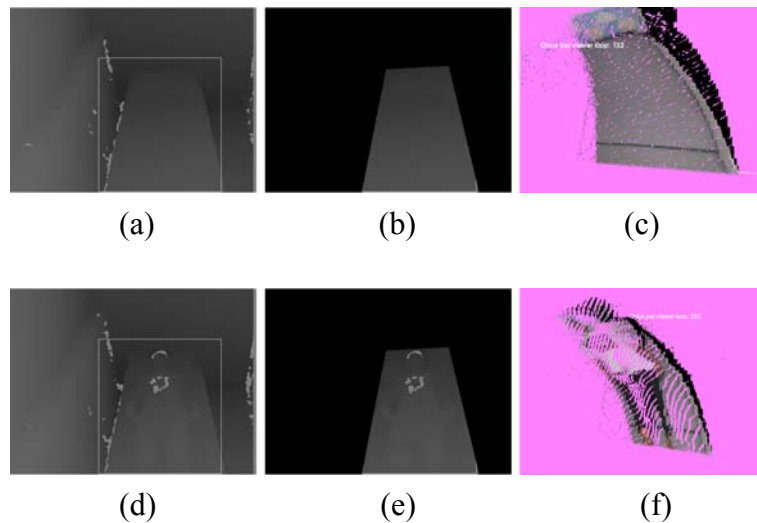


Figure 4.3: World coordinate transformation: (a) Depth image capturing an empty bed, (b) ROI region of the bed, (c) 3D point cloud of the bed; (d) Depth image capturing a subject, (e) ROI region of the subject, (f) 3D point cloud of the subject.

4.3 Experiments on Sleep Posture Recognition

In the section, performance of the method in sleep posture recognition is evaluated. There are three conditions in the experiments: without covering condition, blanket covering condition and quilt covering condition. Finally, results of the three conditions are evaluated.



4.3.1 Experimental Setup

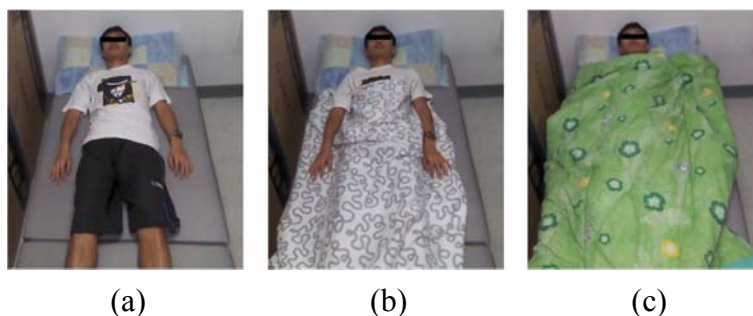


Figure 4.4: Sleep posture experiments in three conditions: (a) Without covering condition, (b) Blanket covering condition and (c) Quilt covering condition.

For evaluating the method of sleep posture recognition, experiments were carried out for recording nature sleep postures of each participant. In the experiments, participants were directed to do sleep postures, including left fetus, left yearner, left log, right fetus, right yearner, right log, soldier, starfish, stomach log and freefaller types of sleep postures. In Figure 4.4, there were three conditions in the experiments: without covering condition, blanket covering condition and quilt covering condition, and participants were asked to do the same sleep postures in the three conditions. Total time of the experiments were about 12 minutes. The samples of 36 subjects included 29 men and 7 women, ranging in age between 20 to 37 years (Age: mean = 24.6, SD = 4; height: mean = 171.4, SD = 8.1; weight: mean = 65.1, SD = 11.4).

Using the sleep browsing system, space of the experiments was set in a room located in the campus. For capturing clear face of subjects, the device (Kinect for Windows) was set at a distance of 50 cm, and in a height above the bed of 135 cm. It set in front of a bed at a depression angle of 20° that the camera view was in the center of a bed covering the entire body of a subject.

4.3.2 Sleep Posture Feature

After the experiments, ten types of sleep postures were recorded. Features of the sleep postures are discussed. In Figure 4.5 and Figure 4.6, the features of obvious curled legs are in the results of left fetus class and right fetus class in the three conditions. In Figure 4.7 and Figure 4.8, the features of

obvious arm shapes are in the results of left yearner class and right yearner class in without covering condition. In blanket covering condition and quilt covering condition, the features of arms stretching out of covering are in the results of left yearner class and right yearner class. In Figure 4.9 and Figure 4.10, the features of both hands sticking on the side of body and obvious rectangle-shaped torso under covering are in the results of left log class and right log class in blanket covering condition and quilt covering condition. In Figure 4.13 and Figure 4.14, the features of separate legs are in the results of soldier class and stomach log class in without covering condition. In blanket covering condition and quilt covering condition, the features of obvious oval-shaped torso are in the results of soldier class and stomach log classes. In Figure 4.13 and Figure 4.14, obvious hands features are in the results of starfish class and freefaller class in the three conditions. Finally, features of ten types of sleep postures were discovered.

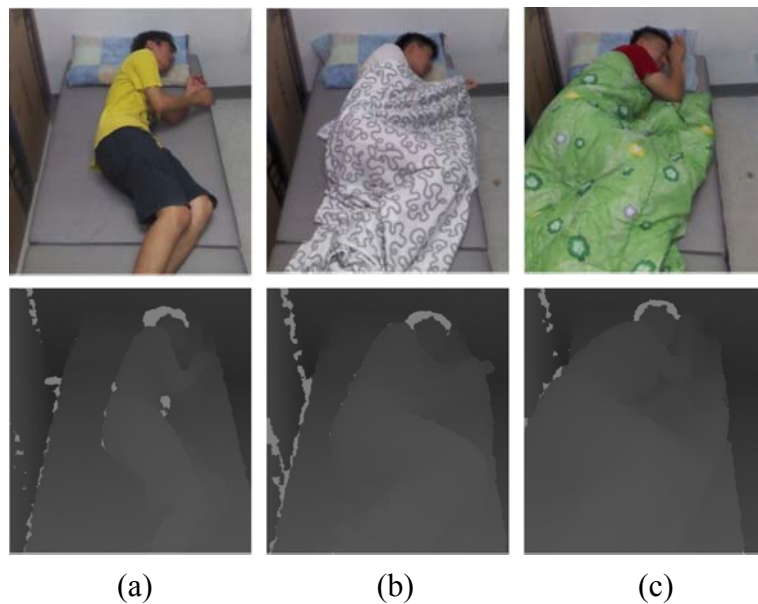
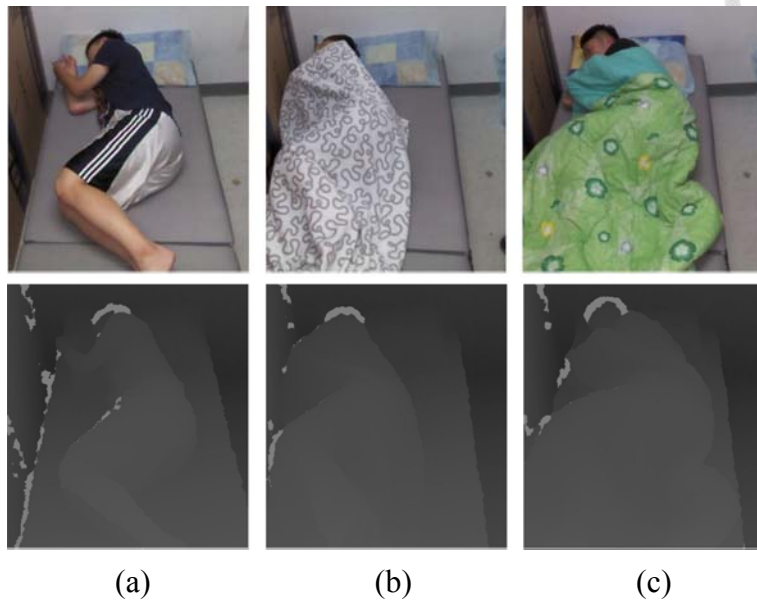
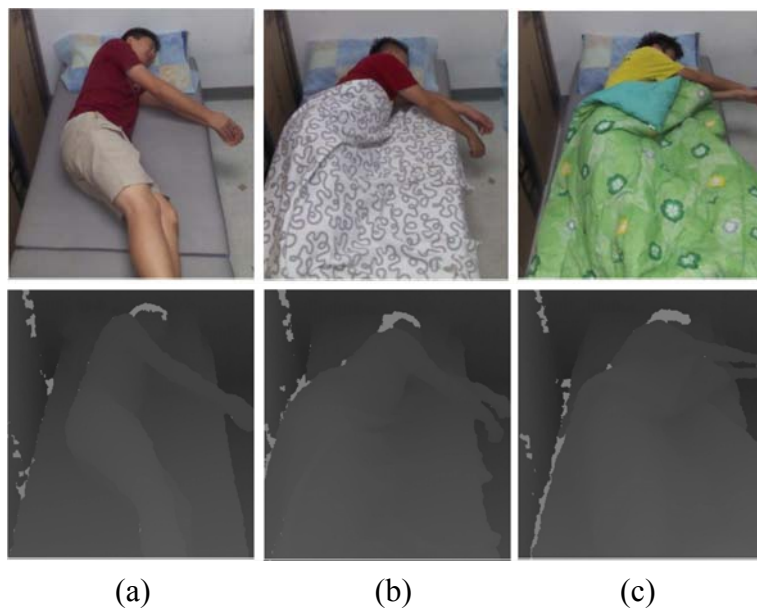


Figure 4.5: Features of left fetus class: (a) User 1 in without covering condition, (b) User 4 in blanket covering condition, and (c) User 11 in quilt covering condition.



(a) (b) (c)
Figure 4.7: Features of right fetus class: (a) User 3 in without covering condition, (b) User 9 in blanket covering condition, and (c) User 10 in quilt covering condition.



(a) (b) (c)
Figure 4.6: Features of left yearner class: (a) User 5 in without covering condition, (b) User 11 in blanket covering condition and (c) User 1 in quilt covering condition.

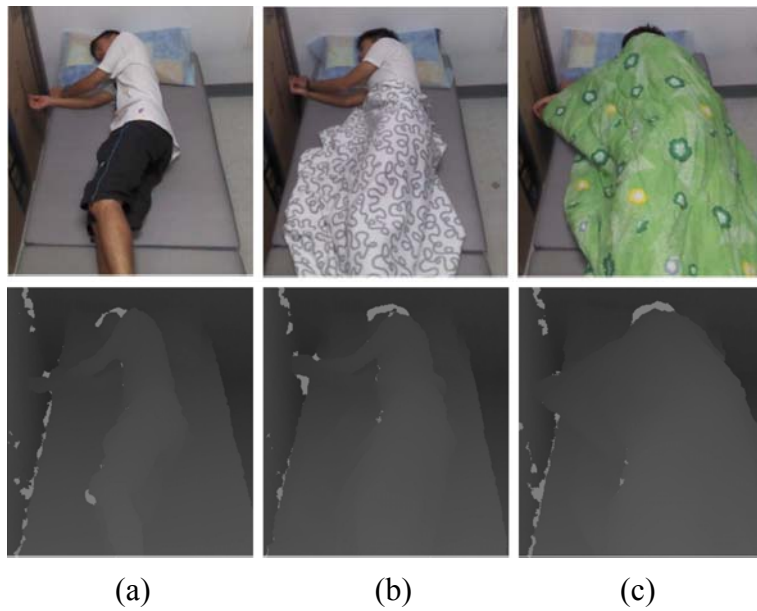


Figure 4.9: Features of right yearner class: (a) User 2 in without covering condition, (b) User 4 in blanket covering condition, and (c) User 10 in quilt covering condition.

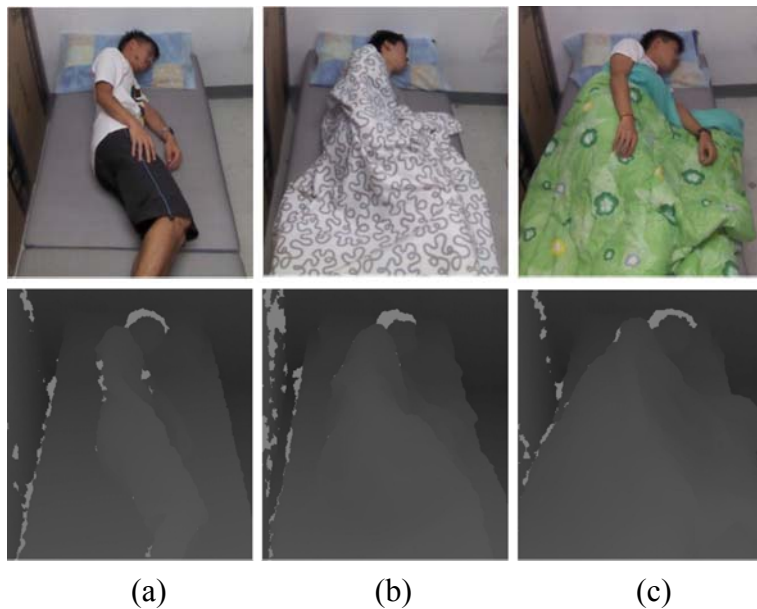
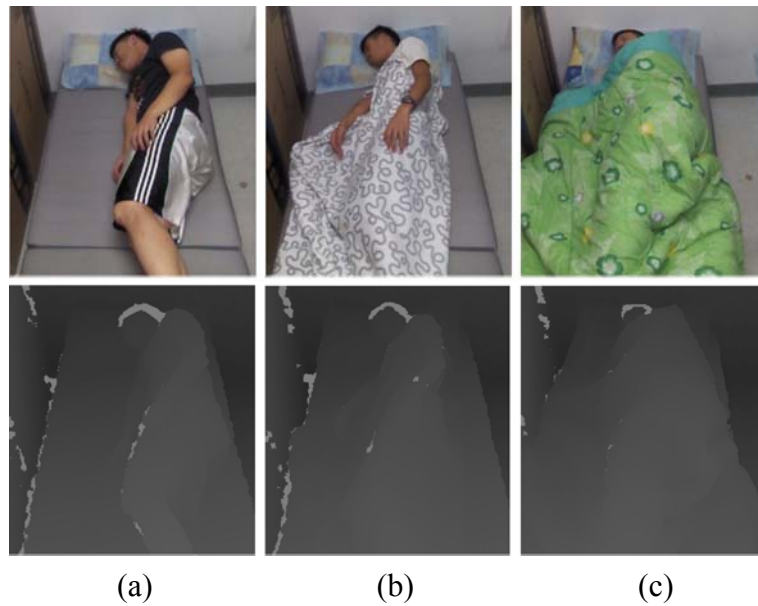
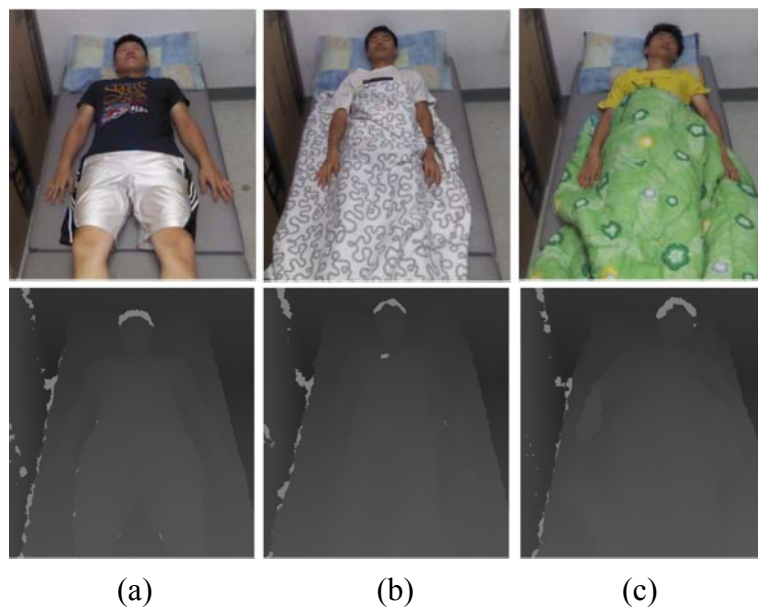


Figure 4.8: Features of left log class: (a) User 2 in without covering condition, (b) User 18 in blanket covering condition and (c) User 4 in quilt covering condition.



(a) (b) (c)
Figure 4.11: Features of right log class: (a) User 3 in without covering condition, (b) User 18 in blanket covering condition and (c) User 9 in quilt covering condition.



(a) (b) (c)
Figure 4.10: Features of soldier class: (a) User 3 in without covering condition, (b) User 2 in blanket covering condition and (c) User 1 in quilt covering condition.

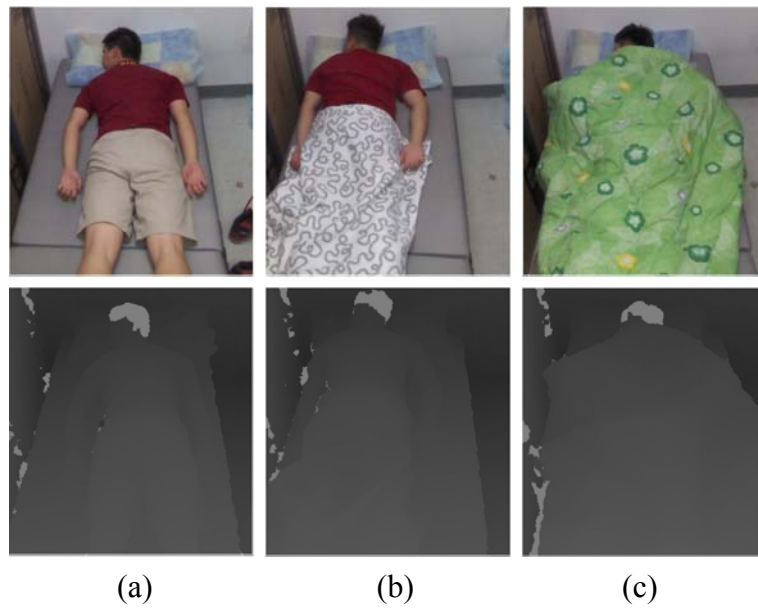


Figure 4.12: Features of stomach log class: (a) User 5 in without covering condition, (b) User 11 in blanket covering condition and (c) User 1 in quilt covering condition.

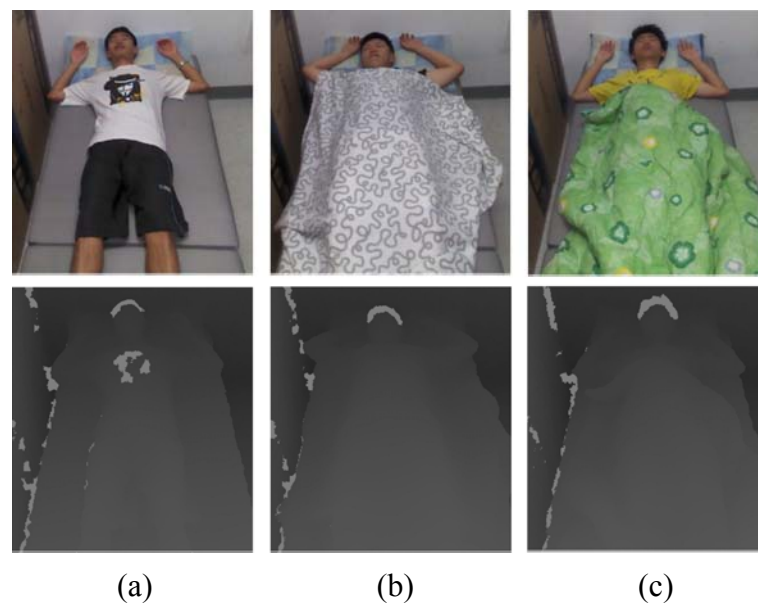


Figure 4.13: Features of starfish class (a) User 2 in without covering condition, (b) User 3 in blanket covering condition and (c) User 1 in quilt covering condition.

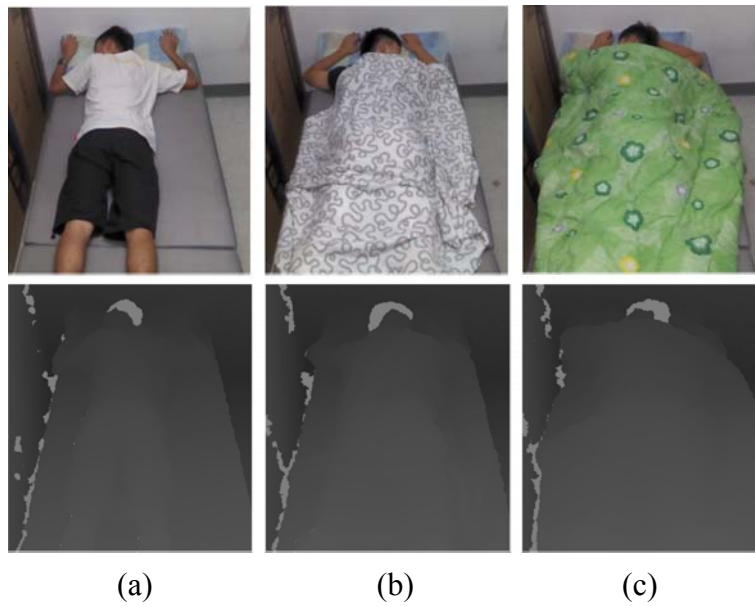


Figure 4.14: Features of freefaller class (a) User 2 in without covering condition, (b) User 3 in blanket covering condition and (c) User 3 in quilt covering condition.

4.3.3 36-fold Cross Validation

Table 4.1: 36-fold cross validation in three conditions.

Condition	Left side (%)	Right side (%)	Supine (%)	Stomach (%)	Average (%)
Without covering	92.39	85.86	66.83	54.88	74.99
Blanket covering	89.38	86.76	71.79	59.24	76.79
Quilt covering	92.08	88.36	74.91	63.82	79.79

Each subset contained 60 depth images to represent each class of sleep postures, and there were total 600 ($60 \times 10 = 600$) samples of each participant. Samples of the 35 participants ($600 \times 35 = 21000$) were used as the training samples to train the model, and samples of the rest 1 participant ($60 \times 10 = 600$) were used as the testing samples. After SVM classification, sleep postures were classified into ten classes: left fetus, left yearner, left log, right fetus, right yearner, right log, soldier, starfish, stomach log and freefaller. The results of left fetus, left yearner and left log classes were considered as left side class, right fetus, right yearner and right log classes were considered as right side class, soldier and starfish classes were considered as supine class, and stomach log and freefaller classes were considered as stomach class.

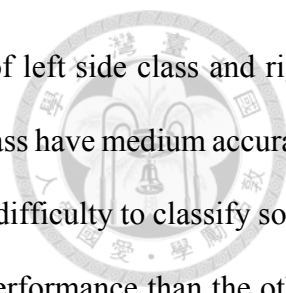


Table 4.1 shows the results of 36-fold cross validation. The results of left side class and right side class have high accuracy, and the results of supine class and stomach class have medium accuracy. For the similarity between supine class and stomach class, the method had difficulty to classify some postures. In addition, the results of quilt covering condition has a better performance than the other two conditions, because the heavy layer of quilt covering enhanced the features of sleep postures.

Without Covering Condition

Table 4.2: 36-fold cross validation in without covering condition.

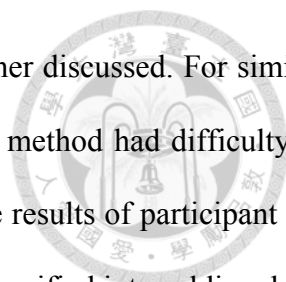
Subjects\ Postures	LF (%)	LY (%)	LL (%)	Left (%)	RF (%)	RY (%)	RL (%)	Right (%)	SD (%)	SF (%)	Supine (%)	SL (%)	FF (%)	Stomach (%)
1	100	100	100	100	100	95	100	98.33	86.67	83.33	85	18.33	18.33	18.33
2	100	100	100	100	100	100	100	100	100	100	100	96.67	100	98.34
3	100	88.33	100	96.11	100	98.33	100	99.44	100	93.33	96.67	100	98.33	99.17
4	81.67	98.33	88.33	89.44	100	100	96.66	98.89	98.33	100	99.17	93.33	3.33	48.33
5	100	100	100	100	100	100	100	100	100	100	100	93.33	41.67	67.5
6	96.67	96.67	100	97.78	95	66.66	100	87.22	6.67	26.67	16.67	93.33	86.67	90
7	100	100	100	100	100	100	98.33	99.44	1.67	3.33	2.5	96.67	100	98.34
8	100	35	50	61.67	100	80	98.33	92.78	0	0	0	100	100	100
9	96.66	98.33	98.33	97.77	100	36.67	8.33	48.33	100	0	50	0	13.33	6.67
10	100	100	100	100	100	100	100	100	0	0	0	25	100	62.5
11	100	96.67	98.33	98.33	100	100	100	100	100	100	100	100	86.67	93.34
12	100	100	100	100	100	3.33	1.67	35	100	100	100	0	0	0
13	100	100	98.33	99.44	93.33	71.67	100	88.33	61.67	0	30.84	1.67	0	0.84
14	100	100	98.33	99.44	100	98.33	100	99.44	100	71.67	85.84	100	100	100
15	100	100	100	100	100	41.67	100	80.56	8.33	8.33	8.33	0	0	0
16	100	100	100	100	100	100	100	100	81.67	0	40.84	85	0	42.5
17	98.33	100	100	99.44	100	0	0	33.33	63.33	0	31.67	96.67	0	48.34
18	100	100	100	100	98.33	100	100	99.44	100	100	100	13.33	0	6.67
19	6.67	100	100	68.89	100	100	98.33	99.44	3.33	13.33	8.33	60	33.33	46.67
20	93.33	100	100	97.78	100	100	1.67	67.22	100	28.33	64.17	100	6.67	53.34
21	98.33	100	100	99.44	100	100	100	100	78.33	73.33	75.83	0	58.33	29.17
22	100	100	100	100	100	100	100	100	100	100	100	0	0	0
23	100	100	100	100	100	100	100	100	100	100	100	76.67	91.67	84.17
24	100	86.66	6.66	64.44	25	96.67	23.33	48.33	40	0	20	11.67	13.33	12.5



Subjects\ Postures	LF (%)	LY (%)	LL (%)	Left (%)	RF (%)	RY (%)	RL (%)	Right (%)	SD (%)	SF (%)	Supine (%)	SL (%)	FF (%)	Stomach (%)
25	100	100	100	100	98.33	91.67	95	95	31.67	48.33	40	100	98.33	99.17
26	100	100	100	100	100	100	100	100	98.33	98.33	98.33	95	60	77.5
27	100	100	100	100	100	100	100	100	100	98.33	99.17	96.67	100	98.34
28	100	100	100	100	100	100	23.34	74.45	98.33	98.33	98.33	23.34	1.67	12.51
29	100	100	98.33	99.44	100	100	98.33	99.44	100	100	100	0	0	0
30	100	100	100	100	100	100	100	100	100	100	100	100	100	100
31	1.67	98.33	0	33.33	83.33	91.67	36.67	70.56	100	100	100	0	26.67	13.34
32	100	100	100	100	100	100	100	100	100	100	100	98.33	100	99.17
33	100	100	100	100	100	100	100	100	100	100	100	45	96.67	70.84
34	0	0	75	25	100	36.66	90	75.55	0	0	0	0	0	0
35	100	100	100	100	6.67	0	0	2.22	100	100	100	100	100	100
36	100	100	95	98.33	100	95	100	98.33	95	13.33	54.17	100	96.67	98.34

*LF: left fetus, LY: left yearner, LL: left log, RF: right fetus, RY: right yearner, RL: right log, SD: soldier, SF: starfish, SL: stomach log, FF: freefaller.

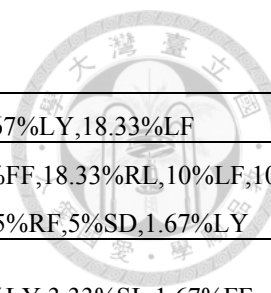
Firstly, results of the methods in without covering condition are discussed. Table 4.2 shows the results of 36-fold cross validation in without covering condition. In left side class, the results of 31 participants (86.11%) have high accuracy, the results of 3 participants (8.33%) have medium accuracy, and the results of 3 participants (8.33%) have low accuracy. In right side class, the results of 30 participants (83.33%) have high accuracy, the results of 1 participant (2.78%) have medium accuracy, and the results of 5 (13.89%) participants have low accuracy. In supine class, the results of 21 participants (58.33%) have high accuracy, the results of 1 participant (2.78%) have medium accuracy, and the results of 14 (38.89%) participants have low accuracy. In stomach class, the results of 16 participants (44.44%) have high accuracy, the results of 2 participants (5.56%) have medium accuracy, and the results of 18 (50%) participants have low accuracy. In without covering condition, the results of left side class and right side class have high accuracy, and the results of supine class and stomach class have medium accuracy.



The results with low accuracy in without covering condition are further discussed. For similar patterns among log posture, soldier posture and stomach log posture, the method had difficulty to classify some postures. In Table 4.3, major postures of left log class in the results of participant 31, and major postures of right log class in the results of participant 12 were classified into soldier class. In Table 4.4, major postures of soldier class were classified into right log class in the results of participant 19, and were classified into stomach log class in the results of participants 6, 10, 15, 25 and 34. Major postures of stomach log class were classified into left log class in the results of participants 18, 21 and 22, were classified into right log class in the results of participant 28, and were classified into soldier class in the results of participants 12 and 31. For similar hand positions between starfish posture and freefaller posture, in Table 4.4, major postures of starfish class were classified into freefaller class in the results of participants 6, 8, 10, 15 and 24, and major postures of freefaller class were classified into starfish class in the results of participants 4, 12 and 19. In addition, efficiency of the method is highly depended on the body proportions of each participant, and that explains the other results with low accuracy showing on Table 4.3 and Table 4.4. From the discussion, the results with low accuracy in without covering condition were caused by the similarity between log and soldier postures, the similarity between starfish and freefaller postures, and differences of body shape and body size.

Table 4.3: Left side class and right side class with low accuracy in without covering condition.

Subjects\ Postures	Left fetus	Left yearner	Left log
31	98.33%SD,1.67%LY		98.33%SD,1.67%SF
34	88.67%RY,11.67%FF,1.67%RL	100%FF	
Subjects\ Postures	Right fetus	Right yearner	Right log
9		61.67%LL,30%RY,6.67%RF,1.67%SL	90%LF,8.33%RY,1.67%SD
12		96.67%SD,3.33%RF	95%SD,3.33%SF,1.67%RL

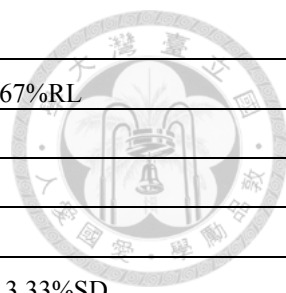


17		91.67%LF,8.33%LL	81.67%LY,18.33%LF
24	41.67%LL,33.33%LF,25%RF		50%FF,18.33%RL,10%LF,10%SF,5%RF,5%SD,1.67%LY
35	68.33%LY,15%LL,10%LF,6.67%RF	98.33%FF,1.67%LY	95%LY,3.33%SL,1.67%FF

*LF: left fetus, LY: left yearner, LL: left log, RF: right fetus, RY: right yearner, RL: right log, SD: soldier, SF: starfish, SL: stomach log, FF: freefaller.

Table 4.4: Supine class and stomach class with low accuracy in without covering condition.

Subjects\ Postures	Soldier	Starfish
6	61.67%SL,31.67%FF,6.67%SF	63.33%FF,26.67%SF,8.33%SL,1.67%RF
7	38.33%LF,33.33%LY,16.67%FF,5%RY,3.33%RL,1.67%LL,1.67%SD	41.67%LF,26.67%RY,20%LY,8.33%RL,3.33%SF
8	53.33%FF,46.67%SL	100%FF
9		100%RL
10	98.33%SL,1.67%RF	100%FF
13		100%SL
15	88.33%SL,8.33%SD,1.67%LY,1.67%LL	91.67%FF,8.33%SF
16		95%SL,5%FF
17		100%LL
19	53.33%RL,21.67%RY,20%LL,3.33%SF,1.67%LF	86.67%RY,13.33%SF
24	41.67%FF,25%SD,15%SF,11.67%SL,6.67%LY	100%FF
25	56.67%SL,31.67%SD,11.67%RY	48.33%SL,45%SD,3.33%RY,3.33%SF
34	100%SL	100%SL
36		36.67%LL,33.33%SL,16.67%RF,13.33%SF
Subjects\ Postures	Stomach log	Freefaller
1	81.67%LF,18.33%SL	71.67%RY,18.33%SL,10%LF
4		96.67%SF,3.33%FF
9	100%RF	86.67%RF,13.33%FF
12	100%SD	100%SF
13	58.33%RY,30%RF,10%RL,1.67%SL	66.67%RY,33.33%RF



15	93.33%LY,5%LF,1.67%RL	78.33%LL,20%LY,1.67%RL
16		100%RL
17		100%LF
18	71.67%LL,15%LF,13.33%FF	75%LF,25%LL
19		63.33%SF,33.33%SL,3.33%SD
20		90%SD,5%SL,3.33%SF,1.67%FF
21	78.33%LL,21.67%LF	45%SL,28.33%LY,13.33%FF,11.67%LF,1.67%SF
22	98.33%LL,1.67%LF	98.33%LL,1.67%RY
24	66.67%LF,15%LL,11.67%FF,6.67%RY	86.67%LF,13.33%FF
28	68.33%RL,11.67%SL,11.67%FF,5%SD,1.67%RY,1.67%SF	96.67%RL,1.67%RF,1.67%FF
29	91.67%LY,8.33%SD	98.33%LY,1.67%SD
31	100%SD	41.67%SD,31.67%SF,26.67%FF
34	100%RF	100%RF

*LF: left fetus, LY: left yearner, LL: left log, RF: right fetus, RY: right yearner, RL: right log, SD: soldier, SF: starfish, SL: stomach log, FF: freefaller.

Blanket Covering Condition

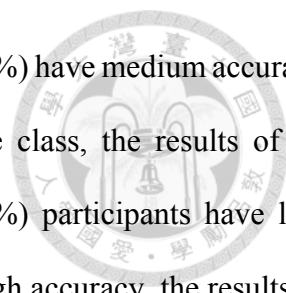
Table 4.5: 36-fold cross validation in blanket covering condition.

Subjects\ Postures	LF (%)	LY (%)	LL (%)	Left (%)	RF (%)	RY (%)	RL (%)	Right (%)	SD (%)	SF (%)	Supine (%)	SL (%)	FF (%)	Stomach (%)
1	100	100	100	100	0	0	3.33	1.11	0	0	0	0	0	0
2	100	100	100	100	100	100	100	100	100	100	100	96.67	100	98.34
3	13.34	3.34	95	37.23	98.33	90	100	96.11	100	100	100	86.67	100	93.34
4	100	98.33	100	99.44	100	98.33	100	99.44	100	100	100	100	100	100
5	100	100	100	100	100	100	100	100	96.67	100	98.34	73.34	18.33	45.84
6	88.34	98.33	98.33	95	88.33	68.34	98.33	85	6.67	0	3.34	45	76.66	60.83
7	100	100	100	100	100	100	100	100	0	3.33	1.67	26.66	93.33	60
8	100	100	100	100	90	100	100	96.67	1.67	81.66	41.67	10	93.33	51.67
9	100	100	100	100	98.33	80	3.34	60.56	100	100	100	15	88.33	51.67
10	100	100	100	100	100	100	100	100	95	96.67	95.84	46.67	98.33	72.5
11	100	100	100	100	100	51.67	100	83.89	100	100	100	75	98.33	86.67
12	6.67	0	100	35.56	100	96.67	100	98.89	95	78.33	86.67	100	78.34	89.17

Subjects\ Postures	LF (%)	LY (%)	LL (%)	Left (%)	RF (%)	RY (%)	RL (%)	Right (%)	SD (%)	SF (%)	Supine (%)	SL (%)	FF (%)	Stomach (%)
13	100	0	88.33	62.78	100	100	88.34	96.11	88.33	8.33	48.33	100	100	100
14	95	100	100	98.33	100	100	100	100	100	95	97.5	95	15	55
15	98.33	98.33	100	98.89	100	53.33	100	84.44	80	81.67	80.84	0	0	0
16	95	100	98.33	97.78	33.33	100	100	77.78	86.67	100	93.34	10	61.67	35.84
17	56.67	96.67	100	84.45	83.33	0	0	27.78	90	0	45	1.67	0	0.835
18	90	100	98.33	96.11	100	100	100	100	0	0	0	100	100	100
19	100	100	100	100	100	100	100	100	100	95	97.5	88.33	60	74.17
20	100	100	100	100	100	96.67	96.67	97.78	100	100	100	5	100	52.5
21	100	100	100	100	100	30	93.33	74.44	100	0	50	0	0	0
22	100	100	100	100	100	93.34	91.67	95	86.67	100	93.34	33.34	65	49.17
23	100	100	100	100	100	100	100	100	100	100	100	8.33	18.34	13.34
24	31.67	100	100	77.22	100	93.33	3.33	65.55	100	0	50	96.67	58.33	77.5
25	41.67	98.33	100	80	100	100	100	100	51.67	100	75.84	85	98.33	91.67
26	100	100	100	100	98.33	46.67	100	81.67	100	93.33	96.67	80	98.33	89.17
27	100	100	98.33	99.44	100	8.33	100	69.44	100	100	100	45	88.33	66.67
28	100	100	93.33	97.78	100	100	100	100	36.66	38.33	37.5	100	96.66	98.33
29	100	0	63.33	54.44	100	100	100	100	10	86.67	48.34	0	0	0
30	100	100	100	100	100	100	95	98.33	100	100	100	100	100	100
31	100	96.66	100	98.89	100	100	100	100	45	100	72.5	18.33	15	16.67
32	100	100	100	100	100	100	100	100	100	100	100	100	96.67	98.34
33	38.33	5	85	42.78	100	100	100	100	96.67	100	98.34	65	36.67	50.84
34	98.33	100	100	99.44	100	98.33	90	96.11	0	0	0	86.67	15	50.84
35	100	13.33	80	64.44	88.33	23.33	0	37.22	100	100	100	100	100	100
36	100	98.33	95	97.78	100	100	100	100	91.67	100	95.84	0	3.33	1.67

*LF: left fetus, LY: left yearner, LL: left log, RF: right fetus, RY: right yearner, RL: right log, SD: soldier, SF: starfish, SL: stomach log, FF: freefaller.

Results of the methods in blanket covering condition are further discussed. Table 4.5 shows the results of 36-fold cross validation in blanket covering condition. In left side class, the results of 30 participants (83.33%) have high accuracy, the results of 2 participants (5.56%) have medium accuracy, and the results of 4 (11.11%) participants have low accuracy. In right side class, the results of 30



participants (83.33%) have high accuracy, the results of 3 participants (8.33%) have medium accuracy, and the results of 3 (8.33%) participants have low accuracy. In supine class, the results of 24 participants (66.67%) have high accuracy, and the results of 12 (33.33%) participants have low accuracy. In stomach class, the results of 16 participants (44.44%) have high accuracy, the results of 3 participants (8.33%) have medium accuracy, and the results of 17 (47.22%) participants have low accuracy. In blanket covering condition, the results of left side class and right side class have high accuracy, and the results of supine class and stomach class have medium accuracy.

The results with low accuracy in blanket covering condition are further discussed. For similar patterns among log posture, soldier posture and stomach log posture, the method also had difficulty to classify some postures in blanket covering condition. In Table 4.6, major postures of left log class were classified into right log class in the results of participant 12, and were classified into stomach log class in the results of participant 33. Major postures of right log class were classified into left log class in the results of participants 17 and 35. In Table 4.7, major postures of soldier class were classified into left log class in the results of participant 1, were classified into right log class in the results of participant 18, and were classified into stomach log class in the results of participants 6, 8, 29 and 34. Major postures of stomach log class were classified into left log class in the results of participant 21, were classified into right log class in the results of participant 1, and were classified into soldier class in the results of participant 29. For the similar hand positions between starfish posture and freefaller posture, major postures of starfish class were classified into freefaller class in the results of participant 13 showing on Table 4.7. The other results with low accuracy were also caused by the different body shapes and body sizes of participants showing on Table 4.6 and Table 4.7. As mentioned previous, the results with low accuracy were caused by the similarity between log and soldier postures, the similarity between starfish and freefaller postures, and differences of body shape and body size.



Table 4.7: Left side class and right side class with low accuracy in blanket covering condition.

Subjects\ Postures	Left fetus	Left yearner	Left log
3	66.67%FF,8.33%SD,8.33%SL,6.67%LF,5%LL,1.67%LY	91.67%FF,3.33%SD,1.67%LF,1.67%LY,1.67%SL	66.67%FF,8.33%SD,8.33%SL,6.67%LF,5%LL,1.67%LY
12	93.33%RL,5%LF,1.67%LL	100%RL	93.33%RL,5%LF,1.67%LL
29		95%SD,5%SL	
33	61.67%SL,38.33%LF	95%SL,5%LY	61.67%SL,38.33%LF
Subjects\ Postures	Right fetus	Right yearner	Right log
1	100%LF	100%LF	68.33%LF,28.33%LY,3.33%RY
17		100%LL	100%LL
35		73.33%LL,13.33%RY,10%RF,3.33%FF	100%LL

*LF: left fetus, LY: left yearner, LL: left log, RF: right fetus, RY: right yearner, RL: right log, SD: soldier, SF: starfish, SL: stomach log, FF: freefaller.

Table 4.6: Supine class and stomach class with low accuracy in blanket covering condition.

Subjects\ Postures	Soldier	Starfish
1	53.33%LL,45%LY,1.67%LF	100%RF
6	58.33%SL,31.67%RY,5%SD,1.67%LF,1.67%SF,1.67%FF	70%RY,30%FF
7	55%FF,43.33%RY,1.67%RL	96.67%RY,3.33%SD
8	33.33%SL,26.67%LL,20%LF,18.33%LY,1.67%SF	
13		91.67%FF,8.33%SD
17		100%LL
18	98.33%RL,1.67%RF	71.67%RF,20%RY,8.33%RL
21		100%LL
24		80%LY,20%SL
28	33.33%SF,28.33%SL,23.33%RL,11.67%RY,3.33%SD	48.33%SL,20%SD,18.33%SF,11.67%RL,1.67%RY



29	90%SL,8.33%SD,1.67%SF	
34	55%SL,45%LF	100%LL
Subjects\ Postures	Stomach log	Freefaller
1	50%RL,48.33%SD,1.67%RY	95%RY,3.33%RL,1.67%SD
5		43.33%RY,38.33%SF,15%FF,3.33%SL
8	45%LF,41.67%RL,10%SL,1.67%LY,1.67%SF	
9	80%LF,15%SL,3.33%SD,1.67%RF	
14		85%RY,15%SL
15	81.67%RY,18.33%LF	85%RY,10%LY,5%LF
16	85%LF,10%SL,5%LY	
17	98.33%LF,1.67%SL	85%LL,15%LF
20	95%LF,5%SL	
21	98.33%LL,1.67%LF	96.67%LL,3.33%LY
22	60%LY,26.67%SL,6.67%RF,6.67%FF	
23	85%SF,5%SL,3.33%RL,3.33%SD,3.33%FF	81.67%RL,16.67%FF,1.67%SL
29	95%SD,5%SF	100%SD
31	81.67%LY,18.33%SL	85%LY,15%SL
33		63.33%RY,36.67%FF
34		81.67%LL,11.67%SL,3.33%LY,3.33%FF
36	100%LY	96.67%LY,3.33%SL

*LF: left fetus, LY: left yearner, LL: left log, RF: right fetus, RY: right yearner, RL: right log, SD: soldier, SF: starfish, SL: stomach log, FF: freefaller.

Quilt Covering Condition

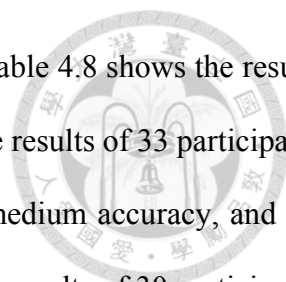
Table 4.8: 36-fold cross validation in quilt covering condition.

Subjects\ Postures	LF (%)	LY (%)	LL (%)	Left (%)	RF (%)	RY (%)	RL (%)	Right (%)	SD (%)	SF (%)	Supine (%)	SL (%)	FF (%)	Stomach (%)
1	100	100	100	100	100	100	100	100	98.33	100	99.17	100	100	100
2	100	100	100	100	100	98.33	95	97.78	100	100	100	50	66.67	58.34
3	51.66	95	100	82.22	100	100	100	100	98.33	100	99.17	100	100	100
4	100	100	100	100	100	100	100	100	100	100	100	100	100	100
5	96.67	1.67	96.66	65	100	100	100	100	0	0	0	0	0	0



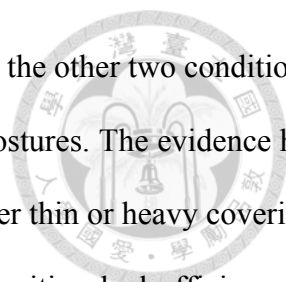
Subjects\ Postures	LF (%)	LY (%)	LL (%)	Left (%)	RF (%)	RY (%)	RL (%)	Right (%)	SD (%)	SF (%)	Supine (%)	SL (%)	FF (%)	Stomach (%)
6	100	100	96.67	98.89	83.33	75.01	53.33	70.56	8.33	0	4.17	66.66	45	55.83
7	100	100	100	100	100	100	100	100	0	46.67	23.34	95	100	97.5
8	100	68.33	100	89.44	100	100	100	100	0	0	0	0	100	50
9	95	15	100	70	70	100	100	90	8.33	0	4.17	0	0	0
10	100	100	98.33	99.44	100	100	100	100	100	100	100	15	78.33	46.67
11	100	100	100	100	100	100	100	100	98.33	100	99.17	36.67	100	68.34
12	100	100	100	100	41.67	3.34	55	33.33	0	63.33	31.67	100	100	100
13	100	100	100	100	100	100	100	100	100	76.66	88.33	100	95	97.5
14	63.33	93.33	100	85.55	100	100	100	100	100	100	100	100	100	100
15	100	100	100	100	83.33	96.67	100	93.33	1.67	100	50.84	60	6.67	33.34
16	100	100	100	100	100	100	100	100	60	98.33	79.17	55	48.34	51.67
17	100	100	100	100	100	93.33	100	97.78	93.33	100	96.67	0	0	0
18	98.33	100	31.67	76.67	83.33	100	100	94.44	86.67	63.34	75.01	98.33	100	99.17
19	100	100	100	100	100	100	100	100	100	21.67	60.84	93.33	100	96.67
20	100	100	35	78.33	100	1.67	5	35.56	100	100	100	68.33	100	84.17
21	100	100	100	100	100	100	100	100	95	98.33	96.67	61.67	100	80.84
22	100	100	100	100	100	100	100	100	100	100	100	91.67	100	95.84
23	100	100	100	100	100	0	100	66.67	96.67	100	98.34	73.34	81.67	77.51
24	100	100	100	100	0	100	5	35	0	0	0	0	1.67	0.84
25	100	100	100	100	65	100	100	88.33	100	100	100	98.33	95	96.67
26	90	95	100	95	95	0	1.67	32.22	100	100	100	48.33	15	31.67
27	100	100	96.67	98.89	98.33	51.67	100	83.33	100	100	100	90	98.33	94.17
28	100	100	100	100	88.33	100	100	96.11	91.67	93.33	92.5	0	8.34	4.17
29	78.33	0	100	59.44	100	100	100	100	0	0	0	0	0	0
30	100	100	93.33	97.78	100	100	100	100	100	100	100	1.67	1.67	1.67
31	100	93.33	100	97.78	100	100	100	100	100	100	100	100	100	100
32	100	100	100	100	100	100	0	66.67	100	100	100	100	100	100
33	100	100	100	100	100	100	100	100	95	100	97.5	100	23.33	61.67
34	0	10	51.67	20.56	100	100	100	100	100	100	100	15	11.67	13.34
35	100	100	100	100	100	100	100	100	100	100	100	100	100	100
36	100	100	100	100	100	100	100	100	100	100	100	100	100	100

*LF: left fetus, LY: left yearner, LL: left log, RF: right fetus, RY: right yearner, RL: right log, SD: soldier, SF: starfish, SL: stomach log, FF: freefaller.



Finally, results of the methods in quilt covering condition are discussed. Table 4.8 shows the results of 36-fold cross validation in quilt covering condition. In left side class, the results of 33 participants (91.67%) have high accuracy, the results of 1 participant (2.78%) have medium accuracy, and the results of 2 (5.56%) participants have low accuracy. In right side class, the results of 30 participants (83.33%) have high accuracy, the results of 2 participants (5.56%) have medium accuracy, and the results of 4 (11.11%) participants have low accuracy. In supine class, the results of 26 participants (72.22%) have high accuracy, the results of 1 participant (2.78%) have medium accuracy, and the results of 9 (25%) participants have low accuracy. In stomach class, the results of 19 participants (52.78%) have high accuracy, the results of 2 participants (5.56%) have medium accuracy, and the results of 15 (41.67%) participants have low accuracy. In quilt covering condition, the results of left side class and right side class have high accuracy, and the results of supine class and stomach class have medium accuracy.

The results with low accuracy in quilt covering condition are further discussed. For the similar patterns among log posture, soldier posture and stomach log posture, the method also had difficulty to classify some postures in quilt covering condition. In Table 4.9, major postures of right log class were classified into soldier class in the results of participant 20, and were classified into stomach log class in the results of participant 26. In Table 4.10, major postures of soldier class were classified into left log class in the results of participant 8, were classified into right log class in the results of participant 9, and were classified into stomach log class in the results of participant 6. Major postures of stomach log class were classified into left log class in the results of participants 26 and 29, were classified into soldier class in the results of participants 10 and 17. For different body shapes and body sizes of participants, the other results with low accuracy are showing on Table 4.9 and Table 4.10. As mentioned previous, the results with low accuracy were caused by the similarity between log and soldier postures, the similarity between starfish and freefaller postures, and differences of body shape and body size.



In quilt covering condition, the results have a better performance than the other two conditions, because the heavy layer of quilt covering enhanced the features of sleep postures. The evidence had shown that the method can be apply in real sleep scenario with subject under thin or heavy covering. Hence, from the experimental results, the method of sleep posture recognition had efficiency to practice in a real sleep scenario with a subject under covering.

Table 4.9: Left side class and right side class with low accuracy in quilt covering condition.

Subjects\ Postures	Left fetus	Left yearner	Left log
29		100%RY	
34	85%RL,13.33%FF,1.67%SF	90%RL,6.67%LL,3.33%LF	51.67%LL,48.33%RL
Subjects\ Postures	Right fetus	Right yearner	Right log
12	58.33%LL,41.67%RF	95%FF,1.67%RY,1.67%RL,1.67%SF	51.67%RF,45%FF,3.33%RY
20		61.67%SD,36.67%SF,1.67%RL	95%SD,5%RL
24	100%LY		86.67%LF,6.67%LL,5%RL,1.67%LY
26		96.67%SL,3.33%LF	75%SL,23.33%LF,1.67%RY

*LF: left fetus, LY: left yearner, LL: left log, RF: right fetus, RY: right yearner, RL: right log, SD: soldier, SF: starfish, SL: stomach log, FF: freefaller.

Table 4.10: Supine class and stomach class with low accuracy in quilt covering condition.

Subjects\ Postures	Soldier	Starfish
5	90%RY,10%RL	86.67%RL,13.33%RY
6	91.67%SL,5%SD,3.33%SF	50%LY,48.33%LL,1.67%SL
7	63.33%FF,35%LY,1.67%RL	51.67%RL,31.67%SF,15%SD,1.67%RY
8	98.33%LL,1.67%LY	96.67%LL,1.67%LF,1.67%LY
9	91.67%RL,8.33%SD	100%RL
12	100%FF	
15	88.33%RY,6.67%LY,1.67%LL,1.67%RF,1.67%SF	
24	100%LF	100%LF
29	100%RF	81.67%RY,18.33%RF

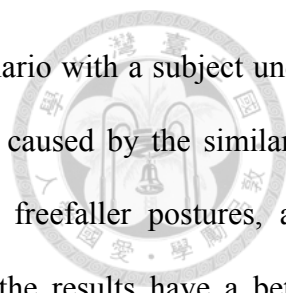


Subjects\ Postures	Stomach log	Freefaller
2	50%SL,38.33%SD,11.67%SF	
5	100%RY	100%RY
6		55%LL,35%FF,10%SL
8	48.33%RF,41.67%LF,10%LL	
9	98.33%RF,1.67%LY	100%RF
10	85%SD,15%SL	
15		55%LY,35%RY,6.67%FF,3.33%LL
16	43.33%SL,26.67%LY,15%LL,11.67%FF,3.33%SD	48.33%SD,46.67%SL,3.33%LY,1.67%FF
17	93.33%SD,3.33%RL,1.67%RY,1.67%SF	96.67%RY,1.67%RL,1.67%SD
24	100%LF	90%LY,8.33%LF,1.67%FF
26	51.67%LL,45%SL,3.33%FF	68.33%SD,16.67%SF,8.33%SL,6.67%FF
28	100%RF	91.67%LL,6.67%FF,1.67%SL
29	88.33%LL,11.67%LF	100%LL
30	98.33%RF,1.67%FF	98.33%RF,1.67%FF
34	85%RF,15%FF	48.33%LL,40%LY,11.67%FF

*LF: left fetus, LY: left yearner, LL: left log, RF: right fetus, RY: right yearner, RL: right log, SD: soldier, SF: starfish, SL: stomach log, FF: freefaller.

4.4 Summary

Unlike other approaches classified sleep postures in the condition of a subject without covering, the benefits and disadvantages of the method in sleep posture recognition has been demonstrated. A framework based of depth image was proposed to transform each depth images into world coordinate, and the vertical distance of each depth pixel to the bed plane was calculated. From the input distance array of each depth image, the SVM method was adopted for classifying four classes of sleep postures: left side, right side, supine and stomach. In the experiments, the method of sleep posture recognition was evaluated in three conditions for simulating real sleep scenario: without covering condition, blanket covering condition and quilt covering condition. From the experimental results, the method



of sleep posture recognition had efficiency to practice in a real sleep scenario with a subject under thin or heavy covering. In addition, the results with low accuracy were caused by the similarity between log and soldier postures, the similarity between starfish and freefaller postures, and differences of body shape and body size. In quilt covering condition, the results have a better performance than the other two conditions, because the heavy layer of quilt covering enhanced the features of sleep postures.



CHAPTER 5

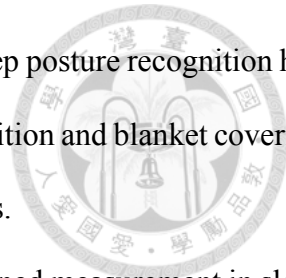
CONCLUSION AND FUTURE WORK

5.1 Summary of the Dissertation

An unconstrained sleep browsing system has been developed for detecting and browsing sleep events in diver sleep environments, and epoch method was proposed for recording three types of sleep events: motion event, lighting event and sound event. Firstly, background modeling in the sleep browsing system was used to measure body movements and lighting changes. Scores of the three types of sleep events were quantified and normalized to the same scale simultaneously. Finally, a browsing interface with sleep diagram was provided for browsing sleep events, presenting the score curves of sleep events and integrated videos. The results of overnight sleep experiments have clearly demonstrated the efficiency and reliability of the sleep browsing system that users browsed the recording of sleep events efficiently, and examined the content of sleep events by watching the videos.

A method of sleep posture recognition based on depth image was proposed for classifying sleep postures into four classes: left side, right side, supine and stomach, in which left side and right side contained fetus, yearner and log types of sleep postures, supine contained soldier and starfish types of sleep postures, and stomach contained log and freefaller types of sleep postures. Firstly, projective coordinate system of each depth image was transformed into world coordinate system. The vertical distance of each depth pixel to the bed plane was calculated. Finally, from the input distance array of each depth image, the SVM method was adopted for classifying sleep postures. Experiments for simulating real sleep scenario with three conditions were carried out: without covering condition,

blanket covering condition and quilt covering condition. The method of sleep posture recognition had a better performance in quilt covering condition than without covering condition and blanket covering condition, because the layer of quilt enhances the features of sleep postures.



Hence, in the study, the sleep browsing system provided an unconstrained measurement in sleep detection, and it is cost-effective for sleep self-examination in home scenario. The method of sleep posture recognition also provided an unconstrained measurement in sleep posture recognition, and it is practical for using in real sleep scenario with a subject under covering.

5.2 Future Directions

Improvement of portable device is helpful for applying the sleep browsing system in home scenario without additional device setting. Smartphones with embedded depth camera has been announced recently, that also brings a possibility to develop the sleep browsing system in mobile application. In addition, the training model of sleep posture recognition can be applied to overnight sleep measurements in the sleep browsing system for real-time sleep posture recognition.



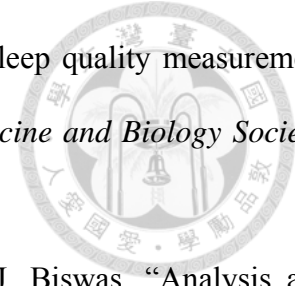
LIST OF REFERENCES

- [1] I. Szollosi, T. Roebuck, B. Thompson and M. T. Naughton, “Lateral sleeping position reduces severity of central sleep apnea / cheyne-stokes respiration,” *Sleep: Journal of Sleep Research & Sleep Medicine*, 29(8), 2006.
- [2] N. A. Eiseman, M. B. Westover, J. M. Ellenbogen and M. T. Bianchi, “The impact of body posture and sleep stages on sleep apnea severity in adults,” *Journal of Clinical Sleep Medicine*, 8(6), 2012, pp. 655-666.
- [3] R. D. Cartwright, “Effect of sleep position on sleep apnea severity,” *Sleep: Journal of Sleep Research & Sleep Medicine*, 7(2), 1984, pp. 110-114.
- [4] “National Sleep Foundation: snoring and sleep,”
<https://sleepfoundation.org/sleep-disorders-problems/other-sleep-disorders/snoring/>.
- [5] R. S. T. Leung, M. E. Bowman, J. D. Parker, G. E. Newton and T. D. Bradley, “Avoidance of the left lateral decubitus position during sleep in patients with heart failure: relationship to cardiac size and function,” *Journal of the American College of Cardiology*, 4(2), 2003, pp. 227-230.
- [6] P.M. Nicassio, D.R. Mendlowitz, J.J. Fussell and L. Petras, “The phenomenology of the pre-sleep state: the development of the pre-sleep arousal scale,” *Journal of Behaviour Research and Therapy* 23(3), 1985, pp. 263-271.
- [7] M.T. Smith, J.A. Haythornthwaite, “How do sleep disturbance and chronic pain inter-relate? Insights from the longitudinal and cognitive-behavioral clinical trials literature,” *Journal of Sleep Medicine Review*, 8(2), 2004, pp. 119-132.
- [8] L. C. L. Chen, K. W. Chen and Y. P. Hung, “A sleep monitoring system based on audio, video



and depth Information for detecting sleep events,” in *Proc. of IEEE International Conference on Multimedia and Expo.*, 2014.

- [9] “National Sleep Foundation: Depression and sleep,” <https://sleepfoundation.org/sleep-disorders-problems/depression-and-sleep/>.
- [10] E. Bixler, “Sleep and society: an epidemiological perspective,” *Journal of Sleep Medicine*, 10, 2009, pp. 1-4.
- [11] K. Asahina, “Paradoxical phase and reverse paradoxical phase in human sleep,” *Journal of Physiological Society of Japan*, 24, 1962, pp. 443-450.
- [12] A. Sano and R.W. Picard, “Toward a taxonomy of autonomic sleep patterns with electrodermal activity,” in *Proc. of IEEE Engineering in Medicine and Biology Society*, 2011.
- [13] R. J. Cole, D. F. Kripke, W. Gruen, D. J. Mullaney and J. C. Gillin, “Automatic sleep/wake identification from wrist actigraphy,” *Sleep: Journal of Sleep Research & Sleep Medicine*, 15, 1992, pp. 461-469.
- [14] F. Wang, M. Tanaka and S. Chonan, “Development of a PVDF piezopolymer sensor for unconstrained in-sleep cardiorespiratory monitoring”, *Journal of Intelligent Material System and Structure*, 14, 2003, pp. 185-200.
- [15] K. Nakajima, K. Matsumoto and T. Tamura, “Development of real-time image sequence analysis for evaluating posture change and respiratory rate of a subject in bed, *Journal of Physiological Measurement*, 22, 2001, pp. N21-N28.
- [16] J. Lee, M. Hong and S. Ryu, “Sleep monitoring system using Kinect sensor,” *International Journal of Distributed Sensor Networks*, 875371, 2015.
- [17] J. Du, C.E. Postma, H.C. Van Vugt and E. Zwartkruis, “Understanding the user needs for sleep enhancement,” Philips Internal Report, 2008.
- [18] K. Z. Siejko and K. R. Maile, “Method for correction of posture dependence on heart sounds,” US Patent 7662104 B2, 2010.



- [19] H. Miwa, S. Sasahara and T. Matsui, "Roll-over detection and sleep quality measurement using a wearable Sensor," in *Proc. of IEEE Engineering in Medicine and Biology Society*, 2007, pp. 1507-1510.
- [20] C. C. Hsia, K. J. Liou, A. P. Aung, V. Foo, W. Huang and J. Biswas, "Analysis and comparison of sleeping posture classification methods using pressure sensitive bed system," in *Proc. of IEEE Engineering in Medicine and Biology Society*, 2009.
- [21] J. Kortelainen and J. Virkkala, "PCA model for recording respiration and posture with multichannel BCG sensor in bed mattress," in *Proc. of International Conference on Wearable, Micro & Nano Technologies for Personalized Health*, 2007.
- [22] M. Papakostas, J. Staud, F. Makedon and V. Metsis, "Monitoring breathing activity and sleep patterns using multimodal non-invasive technologies," in *Proc. of ACM International Conference on Pervasive Technologies Related to Assistive Environments*, 2015.
- [23] Y. Booranrom, B. Watanapa and P. Mongkolnam, "Smart bedroom for elderly using Kinect," in *Proc. of Computer Science and Engineering Conference*, 2014, pp. 427-432.
- [24] M. C. Yu, H. Wu, J. L. Liou, M. S. Lee and Y. P. Hung, "Breath and position monitoring during sleeping with a depth camera," in *Proc. of International Conference on Health Informatics*, 2012.
- [25] A. Taylor, H. Wright and L.C. Lack, "Sleeping-in on the weekend delays circadian phase and increases sleepiness the following week," *Journal of Sleep and Biological Rhythms*, 6(3), 2008, pp. 172-179.
- [26] D.F. Dinges and N.B. Kribbs, "Performing while sleepy: effects of experimentally induced sleepiness," In: T.H. Monk (ed.), *Sleep, Sleepiness and Performance*, Wiley, 1991, pp. 97-128.
- [27] M. R. Opp, "Sleeping to fuel the immune system: mammalian sleep and resistance to parasites," *Journal of BMC Evolutionary Biology*, 9(1), 2009.



- [28] E. Urponen, I. Vuori, J. Hasan and M. Partinen, "Self-evaluations of factors promoting and disturbing sleep: an epidemiological survey in Finland," *Journal of Social Science & Medicine*, 26, 1988, pp. 443-450.
- [29] S. Venn, "It's okay for man to snore: the influence of gender on sleep disruption in couples," *Journal of Social Responsibility*, 12(5), 2007.
- [30] B. H. Jacobson, A. Boolani and D. B. Smith, "Changes in back pain, sleep quality, and perceived stress after introduction of new bedding systems," *Journal of Chiropractic Medicine*, 8(1), 2009, pp. 1-8.
- [31] C. Stauffer and W. Grimson, "Adaptive background mixture models for real-time tracking," in *Proc. of Computer Vision and Pattern Recognition*, 1999, pp. 246-252.
- [32] W. W. Tryon, "Activity measurement in psychology and medicine," New York: Plenum Press, 1991.
- [33] J. B. Webster, D. F. Kripke, S. Messin, and et al., "An activity-based sleep monitor system for ambulatory use," *Sleep: Journal of Sleep Research & Sleep Medicine*, 5(4), 1982, pp. 389-399.
- [34] A. Sadeh, K. M. Sharkey and M. A. Carskadon, "Activity-based sleep/wake identification: an empirical test of methodological issues," *Sleep: Journal of Sleep Research & Sleep Medicine*, 3, 1994, pp. 201-207.
- [35] M. J. Chambers, "Actigraphy and insomnia: a closer look; part 1," *Sleep: Journal of Sleep Research & Sleep Medicine*, 17, 1994, pp. 405-408.
- [36] Y. W. Jan, C. W. Chen, C. M. Yang and S. C. Lin, "Validation of the Chinese version of the pre-sleep arousal scale (PSAS)," *Journal of Archives of Clinical Psychology*, 4(1), 2009, pp. 51-58.
- [37] D. J. Buysse, C. F. Reynolds, T. H. Monk, C. C. Hoch, and et al., "Quantification of subjective sleep quality in healthy elderly men and women using the pittsburgh sleep quality index

(PSQI),” *Sleep: Journal of Sleep Research & Sleep Medicine*, 1991.

- [38] C. H. Bastien, A. Vallieres, C. M. Morin, “Validation of the insomnia severity index as an outcome measure for insomnia research,” *Journal of Sleep medicine*, 2(4), 2001, pp. 297-307.

